

## Supporting Information

### Near-Infrared Circularly Polarized Organic Room Temperature Phosphorescence Based on Chiral Host-Guest Doping Strategy

*Junming Xia<sup>a</sup>, Chenchen Xiong<sup>a</sup>, Songmin Mo<sup>b</sup>, Yongfeng Zhang<sup>a</sup>, Kai Zhang<sup>a</sup>, Gengchen Li<sup>a</sup>, Jianbing Shi<sup>a</sup>, Junge Zhi<sup>c</sup>, Bin Tong<sup>a</sup>, Qinghe Wu<sup>b\*</sup>, Peng Sun<sup>d\*</sup>, Zhengxu Cai<sup>a,e\*</sup>, Yuping Dong<sup>a</sup>*

<sup>a</sup> Beijing Key Laboratory of Construction Tailorable Advanced Functional Materials and Green Applications, School of Materials Science and Engineering, Beijing Institute of Technology, Beijing 100081, China

<sup>b</sup> Department of Chemistry and Key (Guangdong-Hong Kong Joint) Laboratory for Preparation and Application of Ordered Structural Materials of Guangdong, Shantou University, Shantou, Guangdong 515063, China

<sup>c</sup> Key Laboratory of Cluster Science of Ministry of Education, School of Chemistry and Chemical Engineering, Beijing Institute of Technology, Beijing 100081, China

<sup>d</sup> Advanced Research Institute of Multidisciplinary Science, Beijing Institute of Technology, Beijing 100081, China

<sup>e</sup> Tangshan Research Institute, Beijing Institute of Technology, Beijing 100081, China

E-mail: [wuqh@stu.edu.cn](mailto:wuqh@stu.edu.cn); [sunpeng@bit.edu.cn](mailto:sunpeng@bit.edu.cn); [caizx@bit.edu.cn](mailto:caizx@bit.edu.cn)

## Experimental

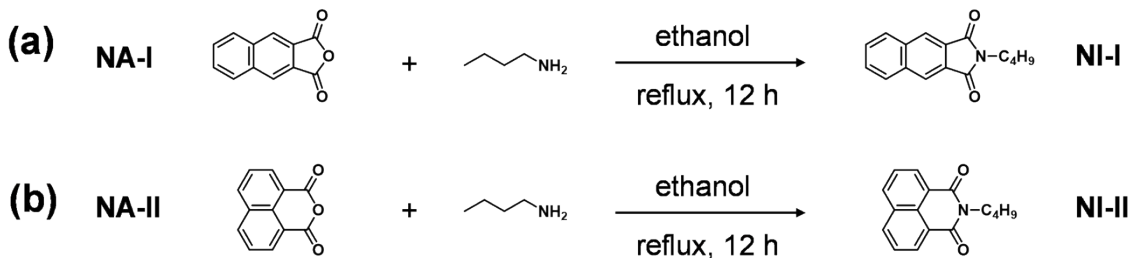
### Materials

Unless otherwise mentioned, all chemicals were obtained from commercial suppliers and used without further purification. The naphthalimide derivative **NI-I**, **NI-II**, **NDI**, **NDI-Br**, **NTI**, and **NTI-Br** were prepared according to the previous work.<sup>[1-6]</sup> (+)-Di-p-toluoyl-D-tartaric acid (D-DTA), (-)-di-p-toluoyl-L-tartaric acid (L-DTA), 2,3-naphthalenedicarboxylic anhydride (NA-I), 1,8-naphthalic anhydride (NA-II), butylamine, etc., were purchased from Meryer Chemical, Energy Chemical, and Beijing Chemworks. Chloroform-*d* was purchased from Energy Chemical. Common solvents, such as dichloromethane (DCM), ethyl acetate, tetrahydrofuran (THF), 1,2-dichloroethane, *N,N*-dimethylformamide (DMF), ethanol, etc., were purchased from Beijing Chemworks.

### Characterization

The <sup>1</sup>H- and <sup>13</sup>C-NMR spectra were measured on a Bruker AV 400 spectrometer. The mass spectra were collected by using a Thermo Q-Extractive mass spectrometer. The UV-Vis absorption spectra were recorded by a UV-2600 UV-Vis spectrophotometer. Fluorescence spectra were measured by a Hitachi F-7000 fluorophotometer. The FLS980 lifetime and steady-state spectrometer were used to determine the phosphorescence spectrum and lifetime. The X-ray crystal structure was measured on a Bruker-AXS SMART APEX2 CCD diffractometer. Intrinsic CPL spectroscopy was investigated using JASCO CPL-200 spectrometer. The J-1500 circular dichroism absorption spectrometer was used to measure the CD spectrum.

## The synthesis of the guest molecules



**Scheme S1.** The synthetic route of NI-I and NI-II.

**NI-I:** NA-I (0.99 g, 5 mmol) was dissolved in ethanol (100 mL), followed by the addition of an excess of n-butylamine (0.40 g, 5.5 mmol), and the reaction was heated with stirring in an oil bath (80 °C) and condensed and refluxed for 12 h. At the end of the reaction, the reaction flask was taken out of the oil bath, and after the reaction solution was naturally cooled down to room temperature, a cyclone was used to remove the ethanol, followed by column chromatography (petroleum ether/dichloromethane, v/v = 1:2) was used to separate the target product NI-I, and its recrystallization to obtain the pure product NI-I (0.57 g, 45.04%). <sup>1</sup>H NMR (400 MHz, chloroform-*d*) δ 8.32 (s, 2H), 8.05 (dd, *J* = 6.2, 3.4 Hz, 2H), 7.69 (dd, *J* = 6.2, 3.3 Hz, 2H), 3.80 – 3.71 (m, 2H), 1.76 – 1.65 (m, 2H), 1.40 (dq, *J* = 14.7, 7.3 Hz, 2H), 0.96 (t, *J* = 7.4 Hz, 3H). <sup>13</sup>C NMR (101 MHz, chloroform-*d*) δ 167.11, 134.36, 129.22, 128.04, 126.87, 123.45, 37.02, 29.57, 19.13, 12.66. MS (ESI) m/z calcd. for C<sub>16</sub>H<sub>15</sub>NO<sub>2</sub> 253.11 [M]<sup>+</sup>, found 254.12 [M+H]<sup>+</sup>.

**NI-II:** NA-II (0.99 g, 5 mmol) was dissolved in ethanol (100 mL), followed by the addition of an excess of n-butylamine (0.40 g, 5.5 mmol), and the reaction was carried out with stirring and heating in an oil bath (80 °C) with condensation and reflux for 12 h. After the reaction was completed, the reaction flask was taken out of the oil bath, and the reaction solution was naturally cooled down to room temperature, and then the solvent ethanol was removed from the reaction solution by using a cyclone. Subsequently, the target product NI-II was separated by column chromatography (petroleum ether/dichloromethane, v/v = 1:2) and recrystallized to obtain the pure product NI-II (0.82 g, 64.79%). <sup>1</sup>H NMR (400 MHz, chloroform-*d*) δ 8.58 (d, *J* = 7.3 Hz, 2H), 8.19 (d, *J* = 8.3 Hz, 2H), 7.79 – 7.67 (m, 2H), 4.24 – 4.12 (m, 2H), 1.71 (p, *J* = 7.6 Hz, 2H), 1.45 (h, *J* = 7.4 Hz, 2H), 0.97 (t, *J* = 7.4 Hz, 3H). <sup>13</sup>C NMR (101 MHz, chloroform-*d*) δ 163.13, 132.77, 130.49, 130.09, 127.04,

125.86, 121.66, 39.20, 29.18, 19.37, 12.84. MS (ESI) m/z calcd. for C<sub>16</sub>H<sub>15</sub>NO<sub>2</sub> 253.11 [M]<sup>+</sup>, found 254.12 [M+H]<sup>+</sup>.

### Preparation of doping materials

For doping powder: Prepare a 150 mg/mL solution of the host-guest mixture in DCM, and raise the temperature to 140 °C in a N<sub>2</sub> atmosphere, and crystallize the material to form doping material after the removal of DCM.

For doping crystalline film: Prepare a 150 mg/mL solution of the host-guest mixture in DCM, and take 130 μL of the solution by pipetting gun and evenly cover it on a 10 × 10 × 1 mm high-purity quartz glass substrate, and place it in a dry room temperature environment. After the solvent volatilizes naturally, the doped material slowly crystallizes to form a CPL crystal film.

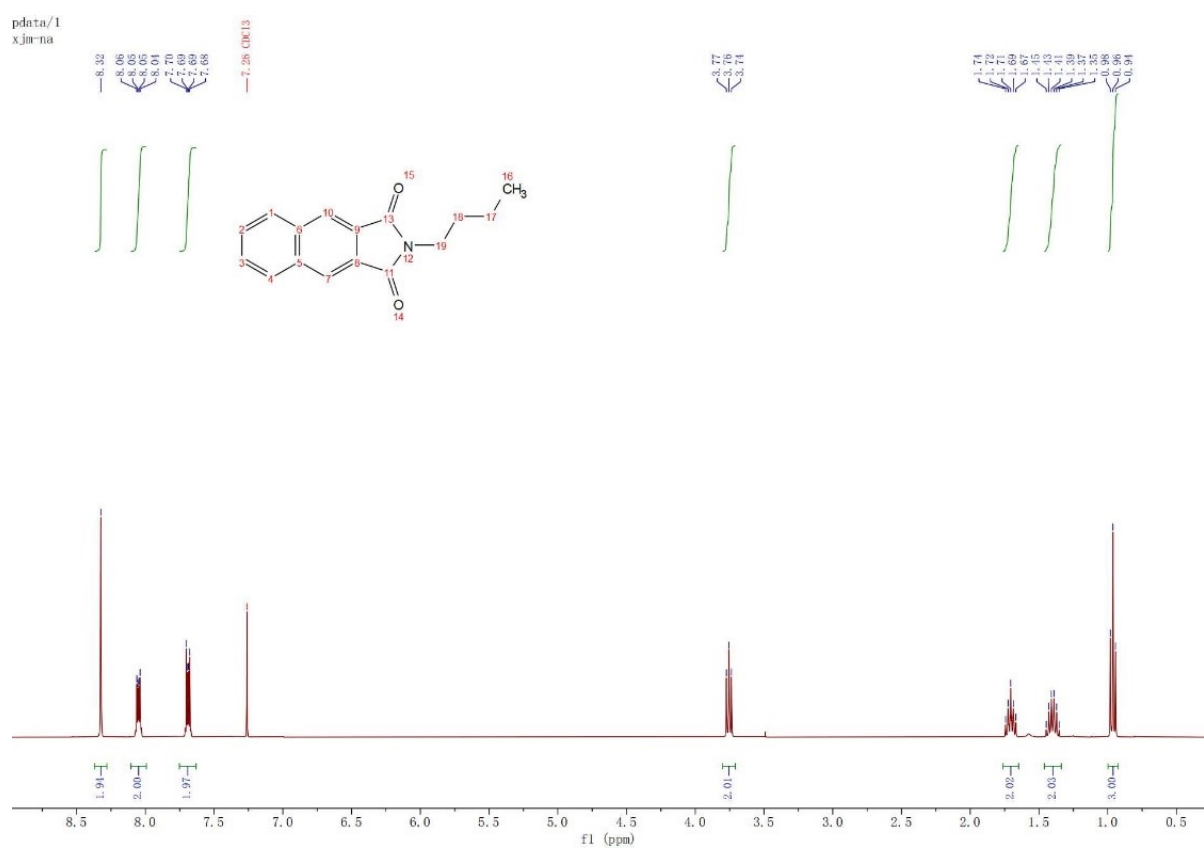


**Figure S1.** The <sup>1</sup>H-NMR spectrum of NI-I in CDCl<sub>3</sub>.

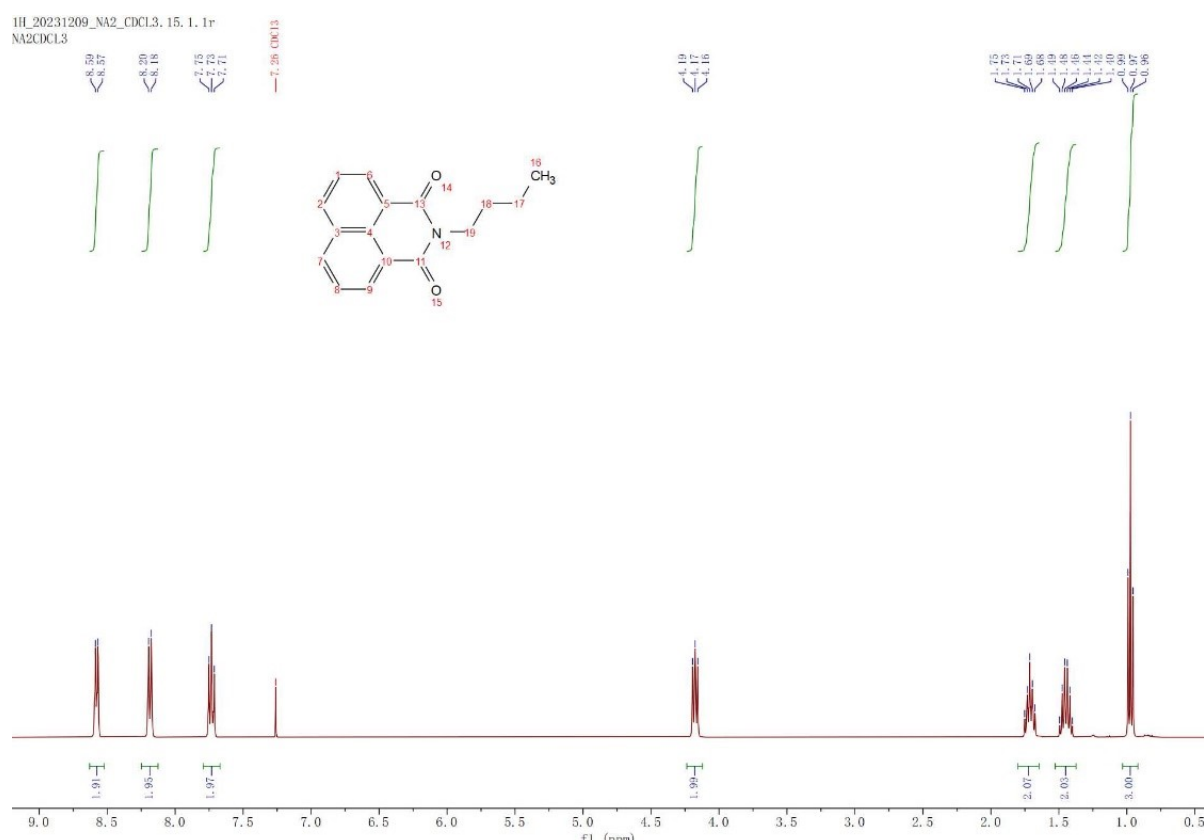


**Figure S2.** The  $^1\text{H}$ -NMR spectrum of **NI-II** in  $\text{CDCl}_3$ .

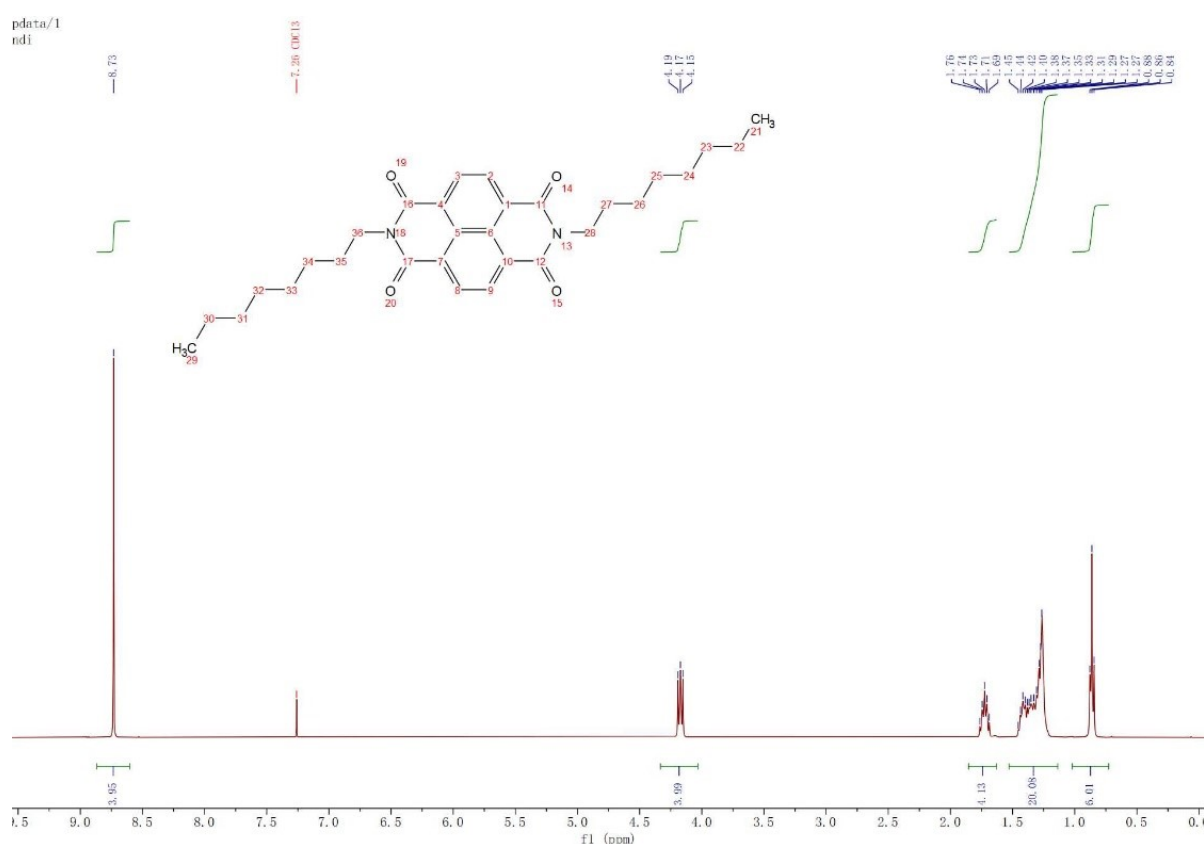


**Figure S3.** The  $^1\text{H}$ -NMR spectrum of NDI in  $\text{CDCl}_3$ .

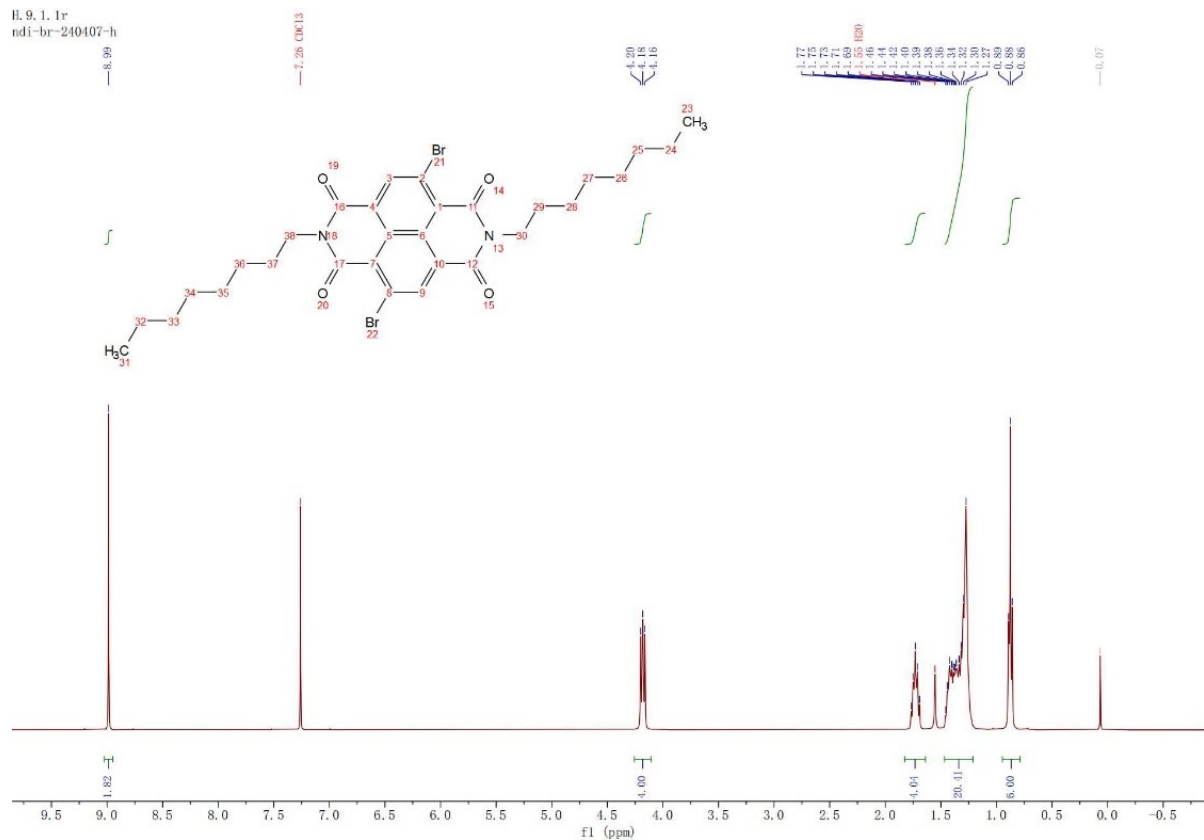


**Figure S4.** The  $^1\text{H}$ -NMR spectrum of **NDI-Br** in  $\text{CDCl}_3$ .

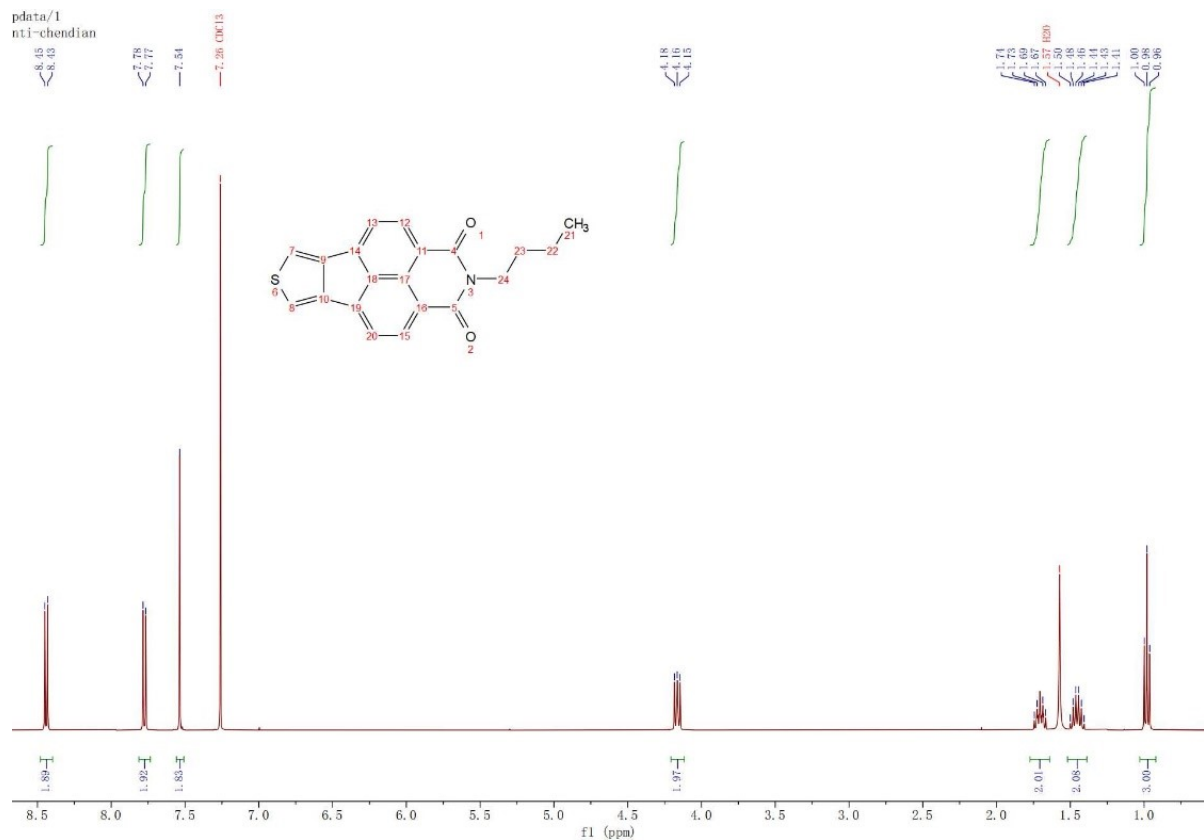


**Figure S5.** The  $^1\text{H}$ -NMR spectrum of NTI in  $\text{CDCl}_3$ .

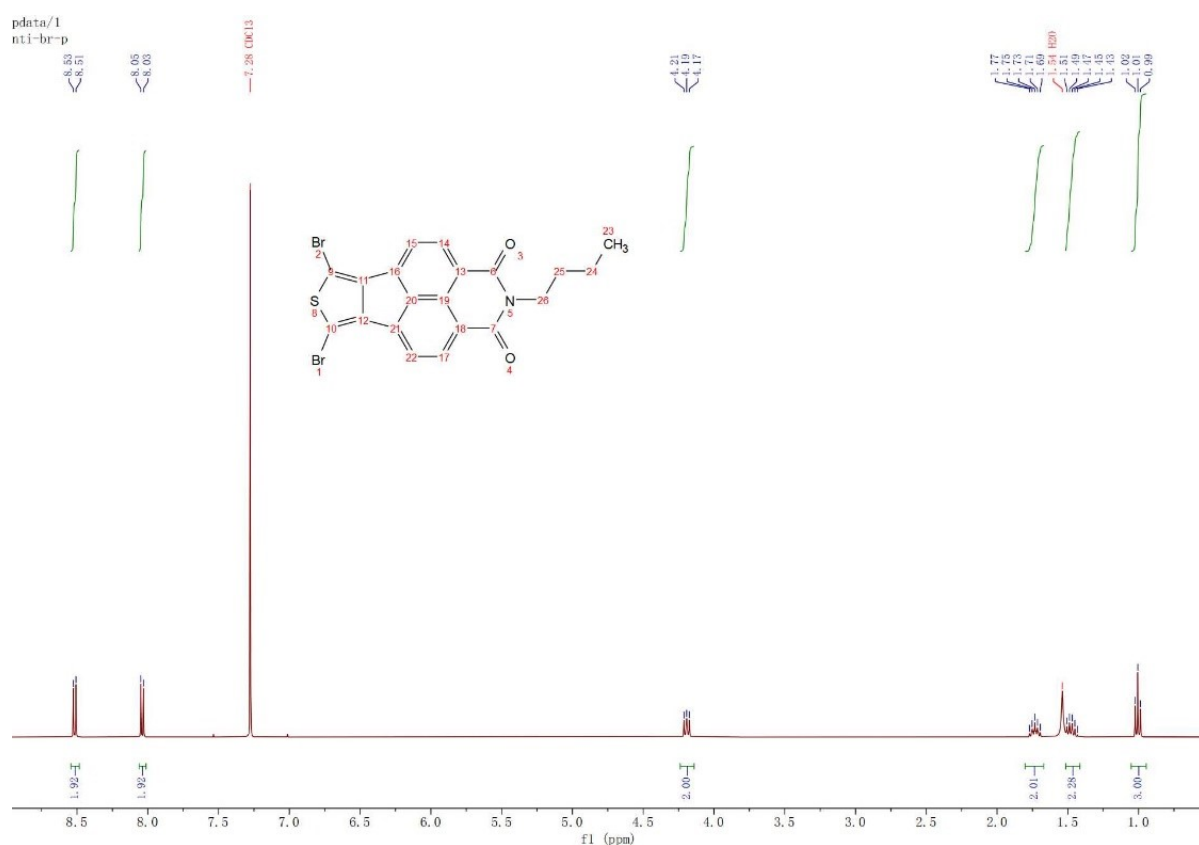


**Figure S6.** The  $^1\text{H}$ -NMR spectrum of NTI-Br in  $\text{CDCl}_3$ .

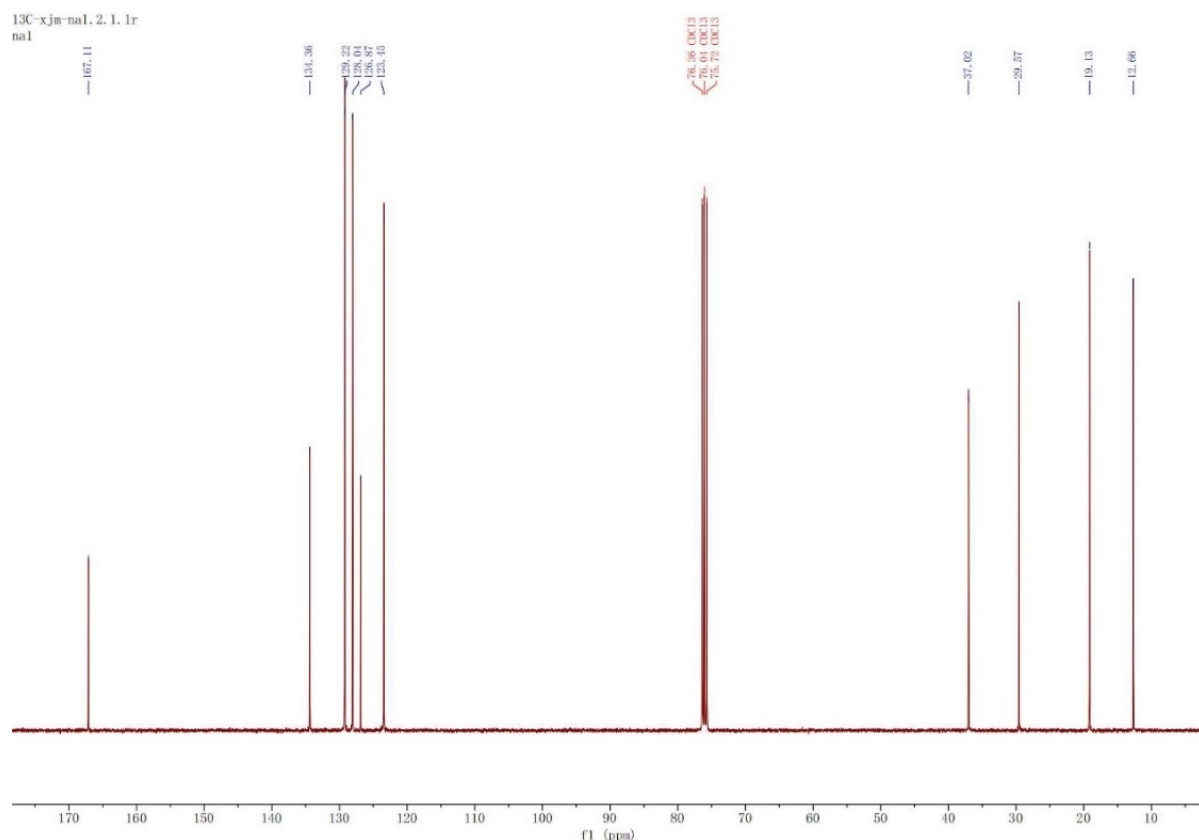


**Figure S7.** The  $^{13}\text{C}$ -NMR spectrum of NI-I in  $\text{CDCl}_3$ .

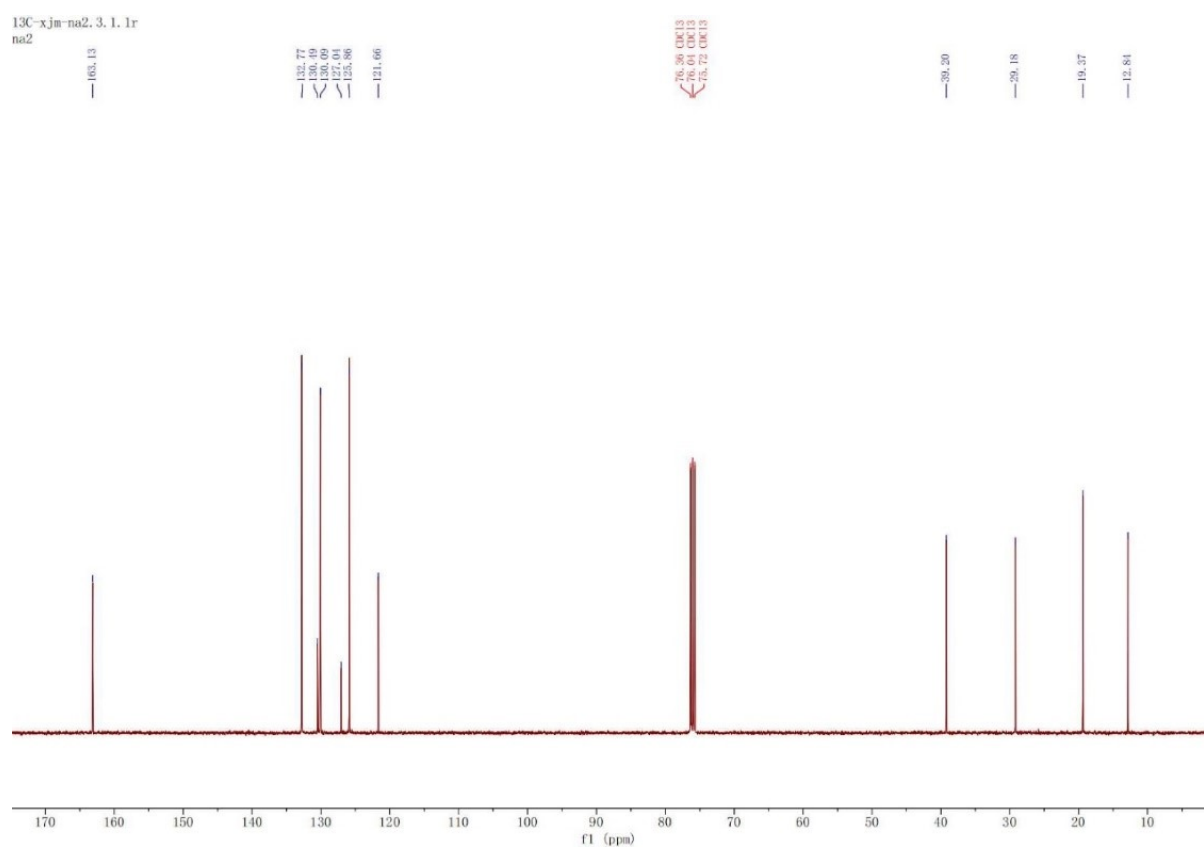


**Figure S8.** The <sup>13</sup>C-NMR spectrum of **NI-II** in CDCl<sub>3</sub>.

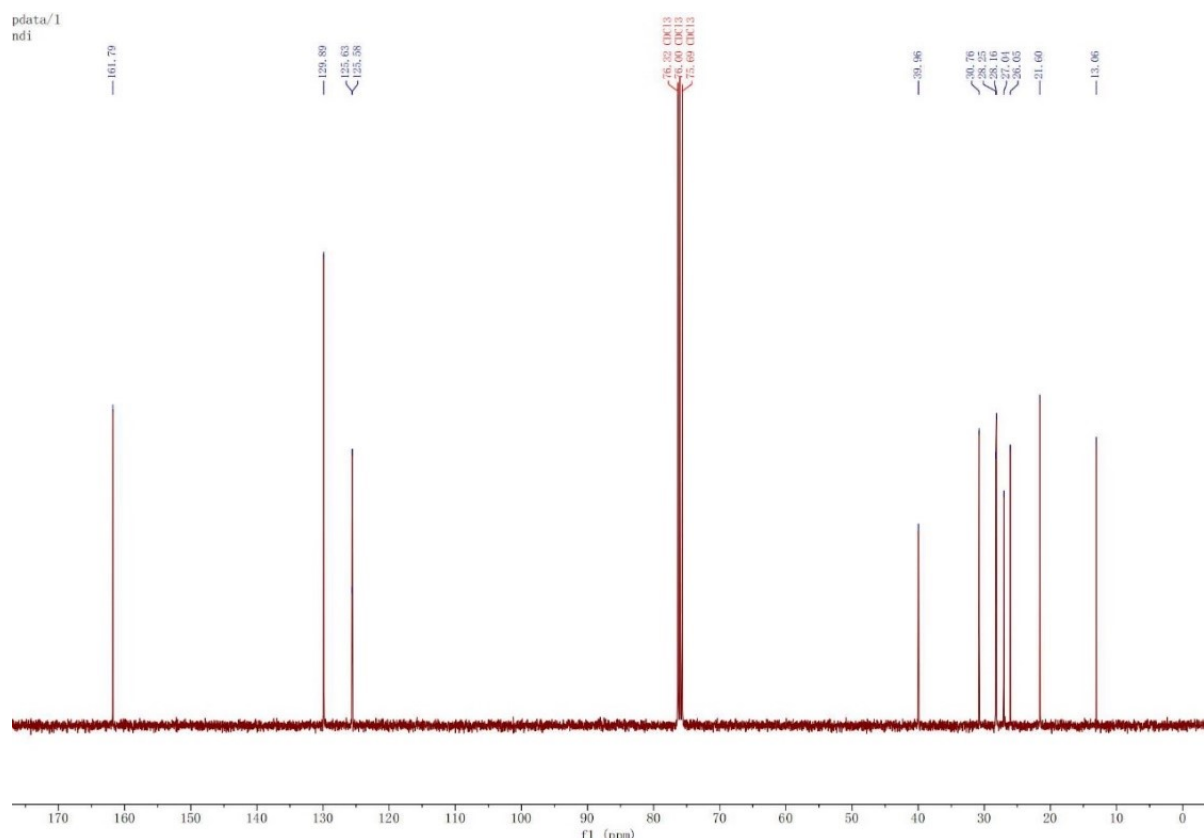


**Figure S9.** The <sup>13</sup>C-NMR spectrum of **NDI** in CDCl<sub>3</sub>.

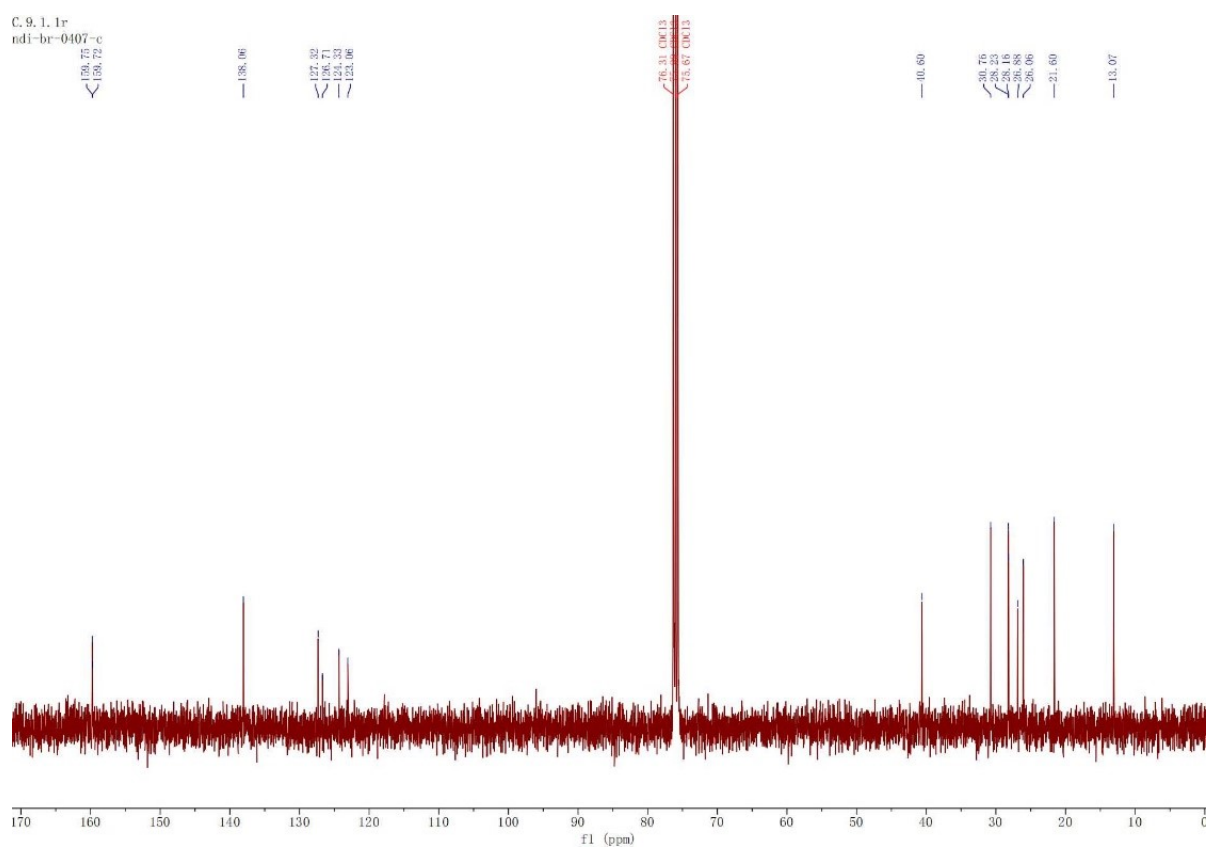


**Figure S10.** The <sup>13</sup>C-NMR spectrum of **NDI-Br** in CDCl<sub>3</sub>.

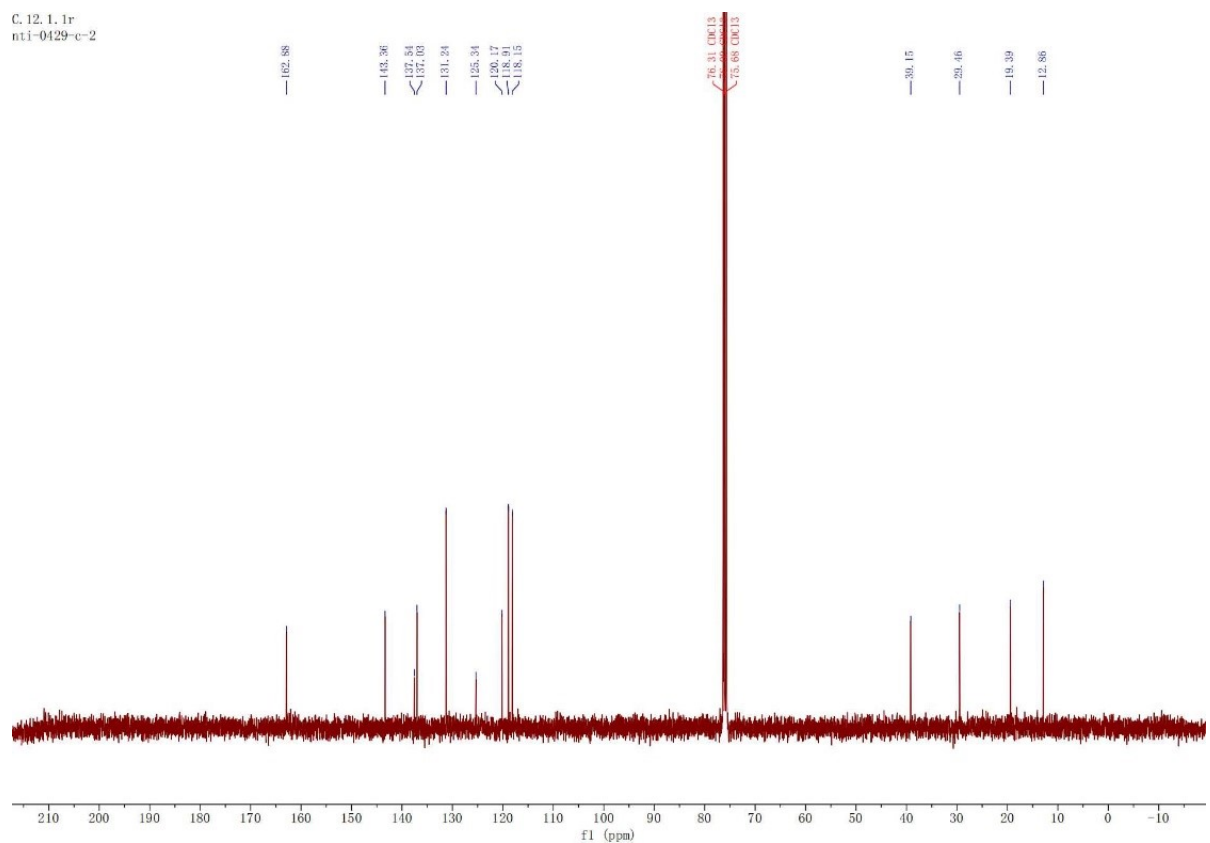


**Figure S11.** The <sup>13</sup>C-NMR spectrum of **NTI** in CDCl<sub>3</sub>.

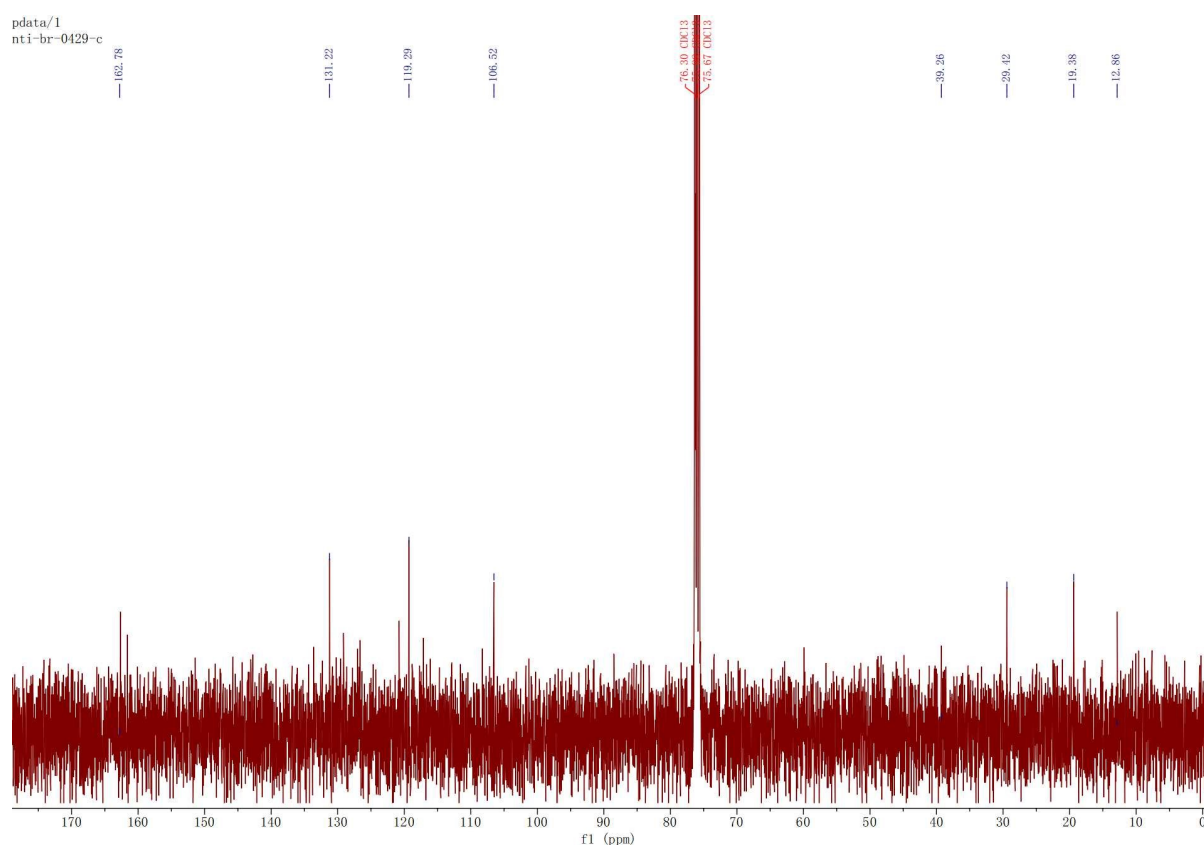


**Figure S12.** The  $^{13}\text{C}$ -NMR spectrum of **NTI-Br** in  $\text{CDCl}_3$ .

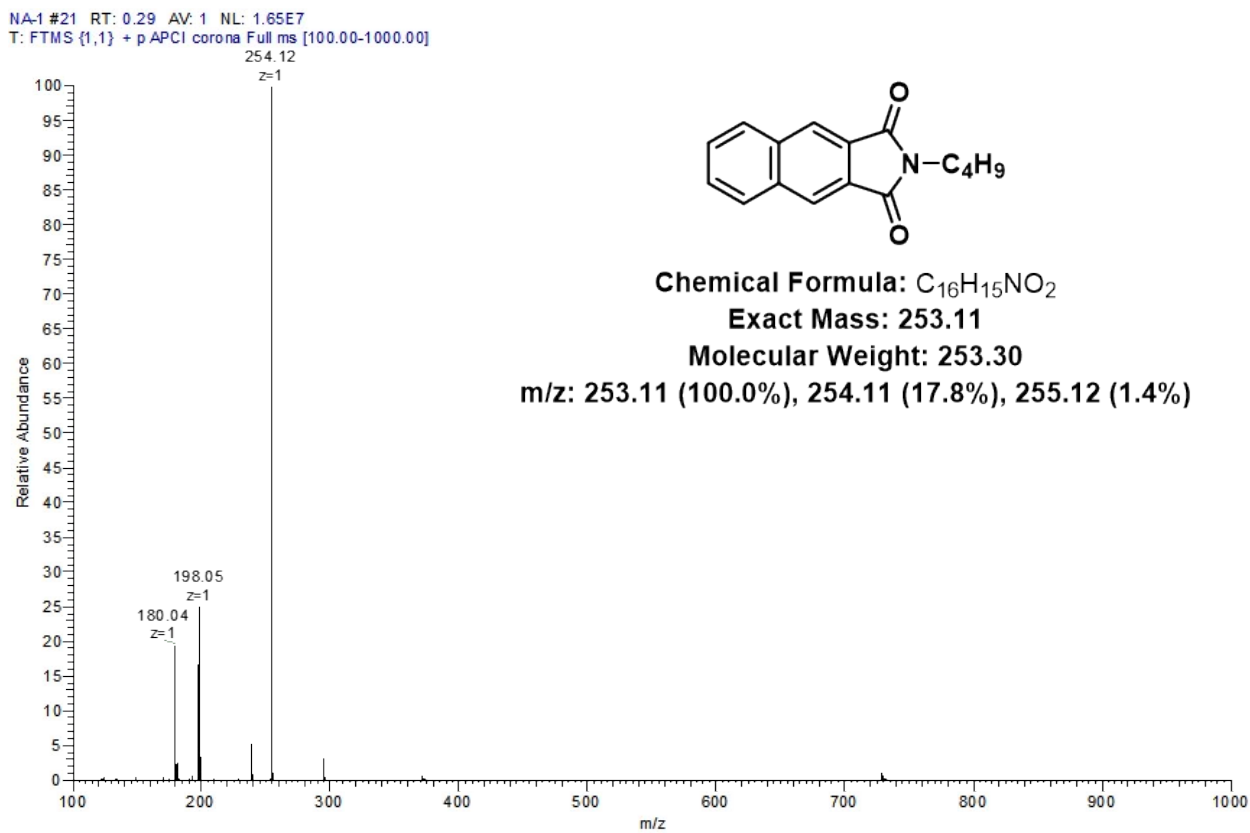


**Figure S13.** The mass spectrum of **NI-I**.

NA-2 #21 RT: 0.29 AV: 1 NL: 2.81E7  
T: FTMS {1,1} + p APCI corona Full ms [100.00-1000.00]

254.12

z=1

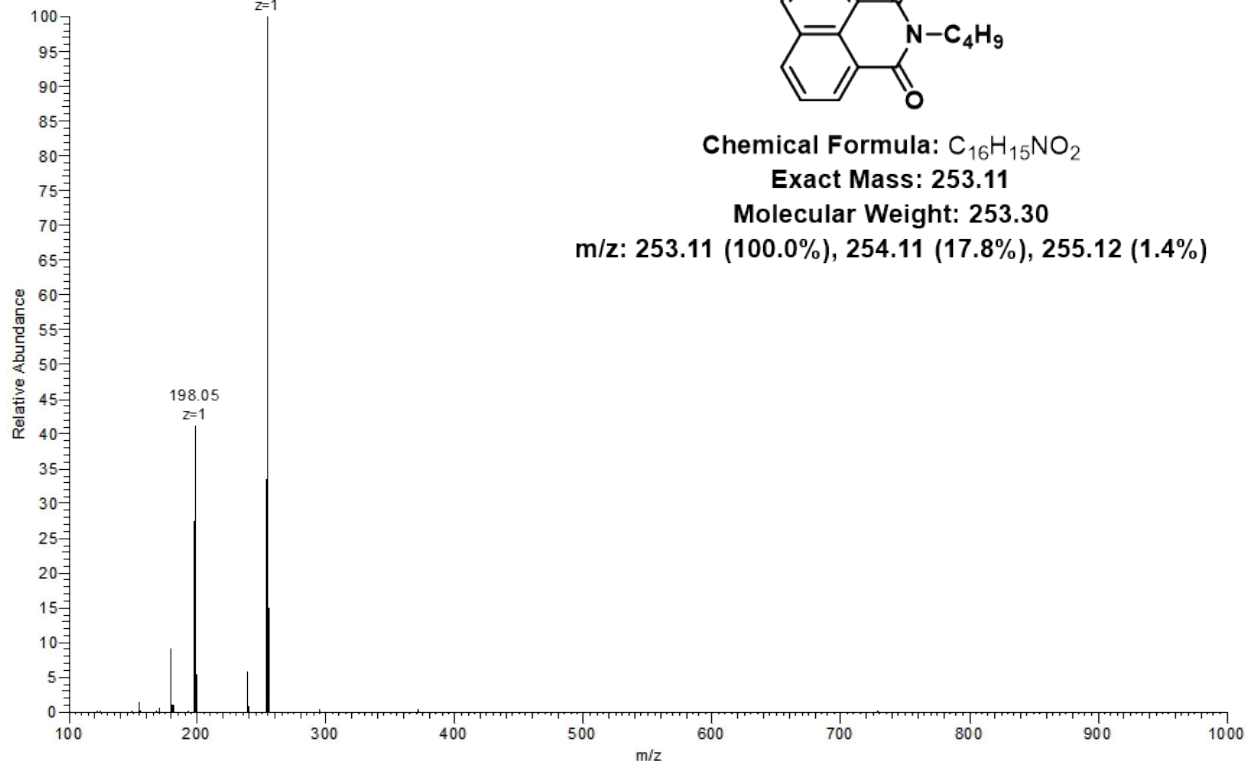
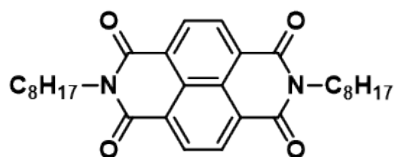


**Figure S14.** The mass spectrum of NI-II.

NDI#13 RT: 0.15 AV: 1 NL: 2.13E7  
T: FTMS {1,1} + p APCI corona Full ms [100.00-1000.00]

491.29

z=1



**Chemical Formula:** C<sub>30</sub>H<sub>38</sub>N<sub>2</sub>O<sub>4</sub>

**Exact Mass:** 490.28

**Molecular Weight:** 490.64

**m/z:** 490.28 (100.0%), 491.29 (33.0%), 492.29 (6.1%)

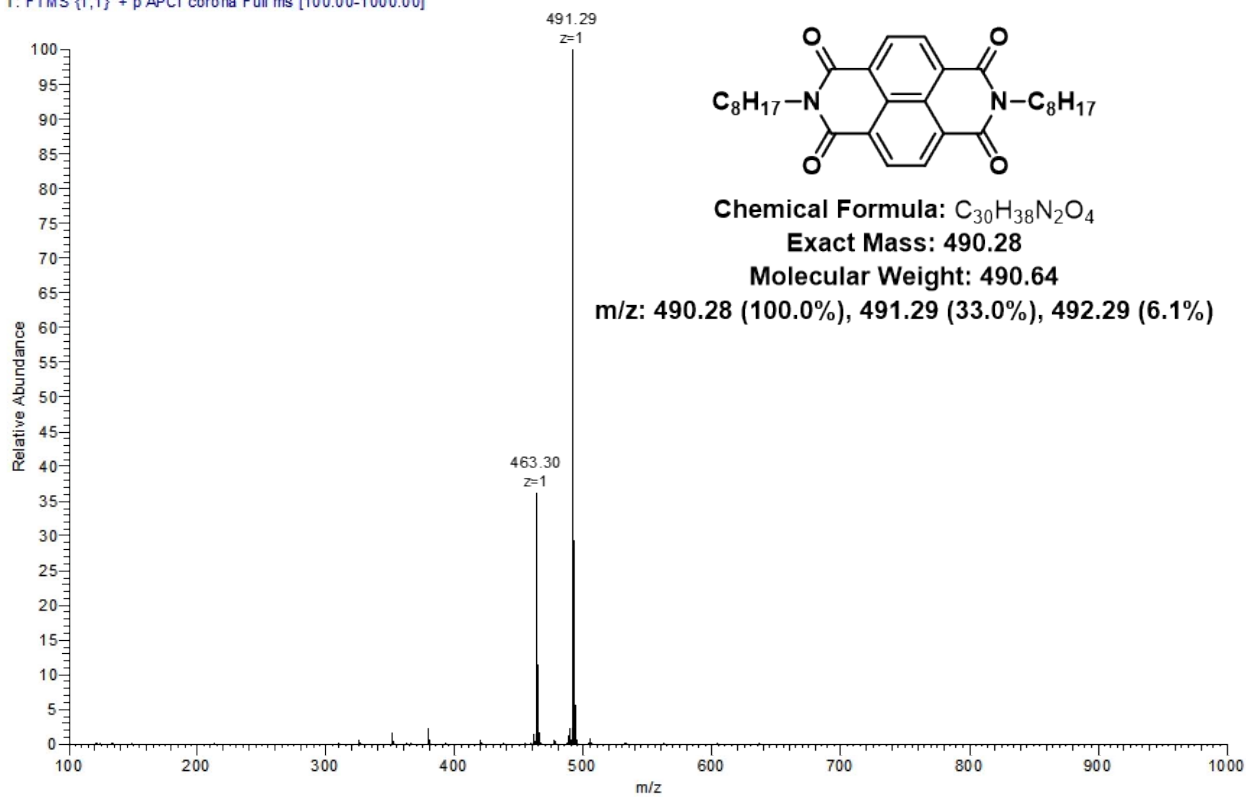


**Figure S15.** The mass spectrum of NDI.

NDI-Br #5 RT: 0.06 AV: 1 NL: 3.25E 6  
T: FTMS {1,1} + p APCI corona Full ms [100.00-1000.00]

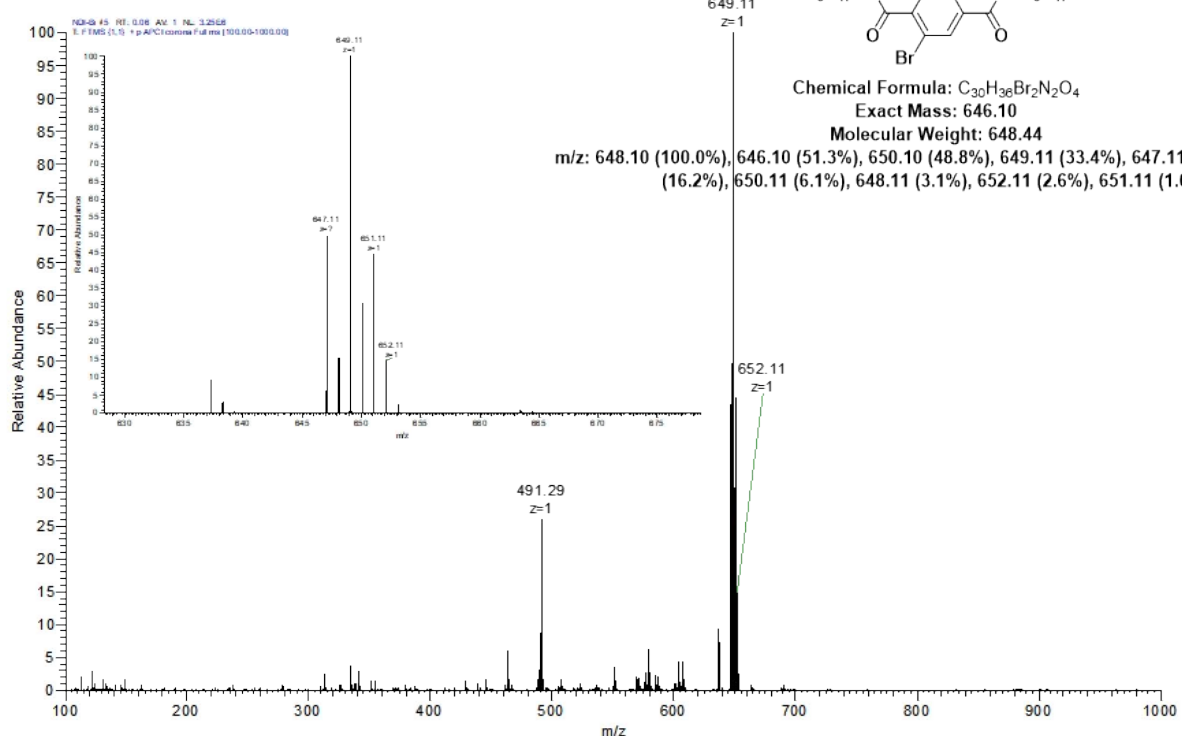


Figure S16. The mass spectrum of NDI-Br.

NTI #7 RT: 0.08 AV: 1 NL: 9.83E7  
T: FTMS {1,1} + p APCI corona Full ms [100.00-1000.00]

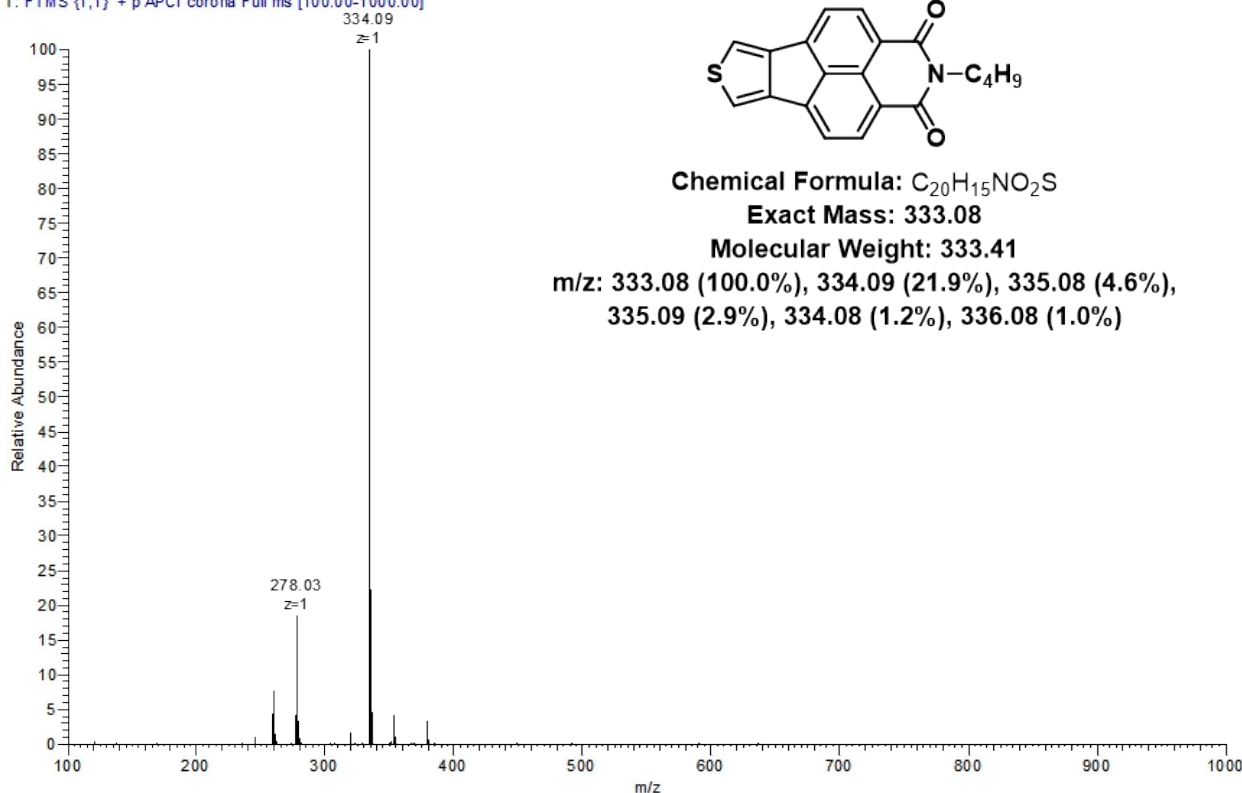
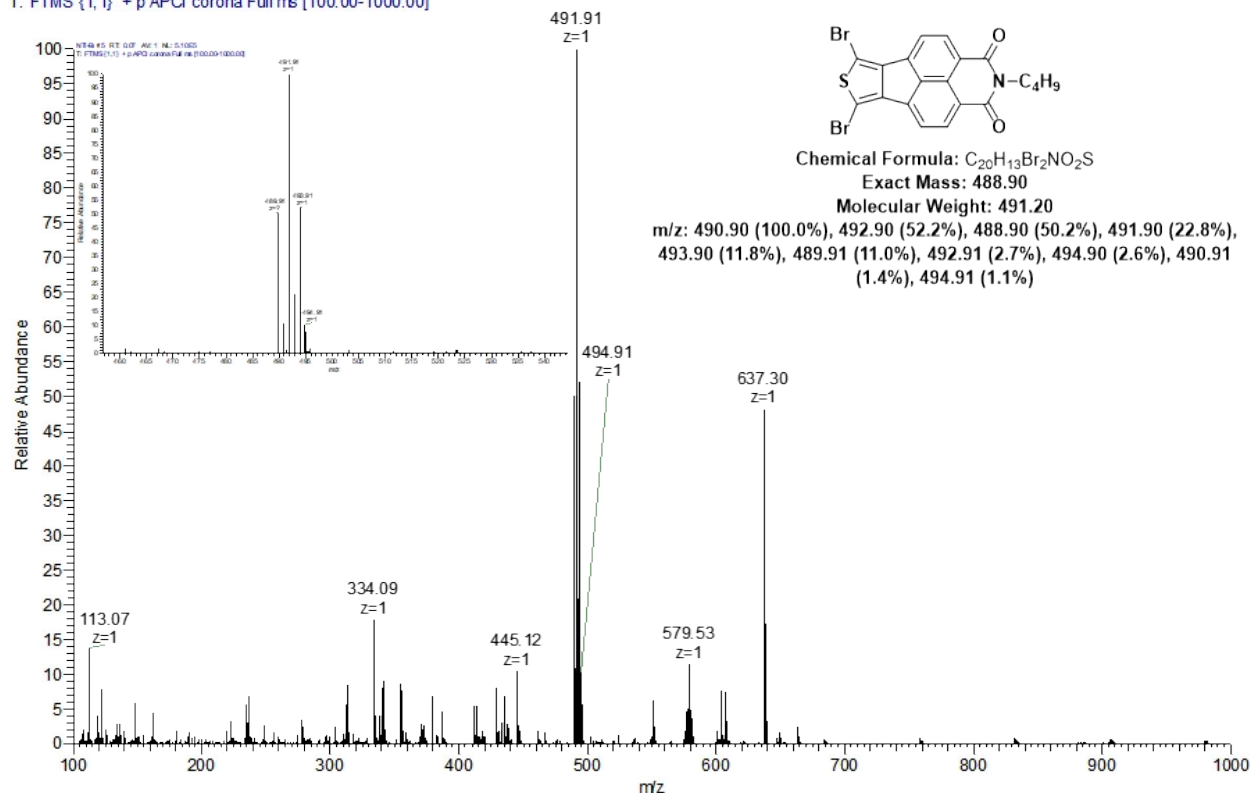


Figure S17. The mass spectrum of NTI.

NTI-Br #5 RT: 0.07 AV: 1 NL: 5.10E5  
T: FTMS {1,1} + p APCI corona Full ms [100.00-1000.00]



**Figure S18.** The mass spectrum of NTI-Br.

**Table S1.** The spin-orbit coupling constant calculation results of guests

State	NI-I ( $\text{cm}^{-1}$ )	NI-II ( $\text{cm}^{-1}$ )	NDI ( $\text{cm}^{-1}$ )	NDI-Br ( $\text{cm}^{-1}$ )	NTI ( $\text{cm}^{-1}$ )	NTI-Br ( $\text{cm}^{-1}$ )
$S_1 \rightarrow T_1$	0.05	14.69	0.00	0.12	0.03	0.00
$S_1 \rightarrow T_2$	0.01	7.61	0.00	0.14	0.00	0.10
$S_1 \rightarrow T_3$	7.47	0.08	0.09	2.62	0.00	0.01
$S_1 \rightarrow T_4$	0.02	15.97	0.00	0.06	4.33	11.30
$S_1 \rightarrow T_5$	0.01	3.25	13.15	274.61	0.00	0.00
$S_1 \rightarrow T_6$	0.08	10.77	0.00	38.00	0.03	0.00
$S_1 \rightarrow T_7$	1.53	1.40	14.37	0.05	0.01	0.04
$S_1 \rightarrow T_8$	0.00	2.78	9.34	229.13	6.34	0.81
$S_1 \rightarrow T_9$	0.06	12.74	0.00	0.03	0.08	0.00
$S_1 \rightarrow T_{10}$	4.14	8.11	0.00	356.54	0.00	69.17

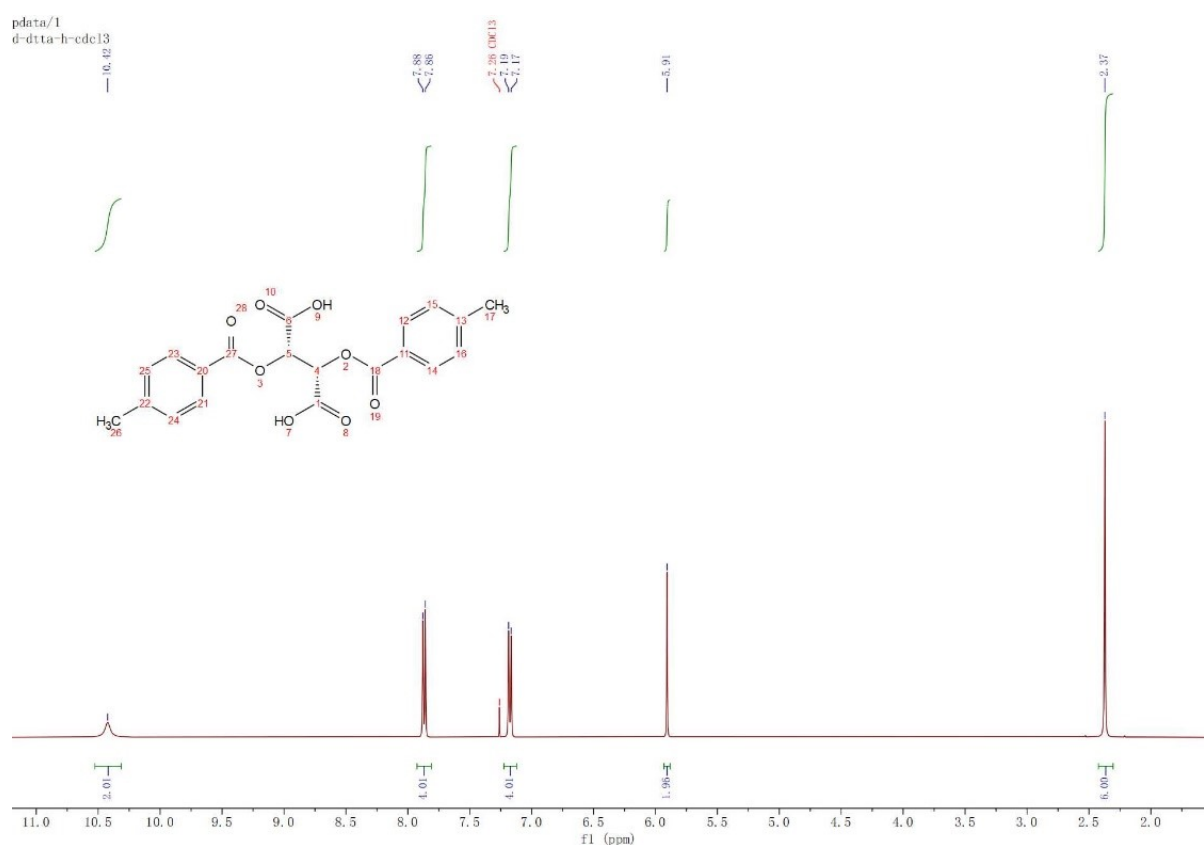


**Figure S19.** The  $^1\text{H}$ -NMR spectrum of **D-DTA** in  $\text{CDCl}_3$ .

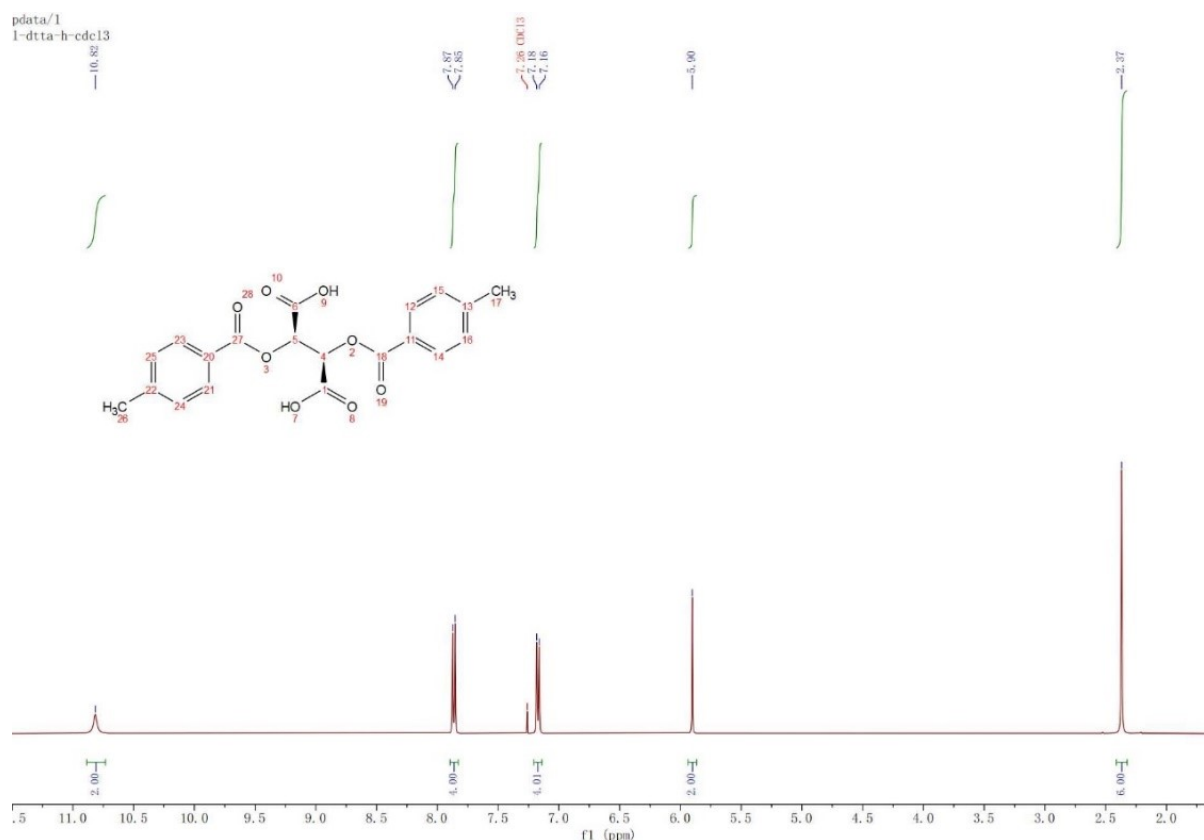


**Figure S20.** The  $^1\text{H}$ -NMR spectrum of **L-DTA** in  $\text{CDCl}_3$ .

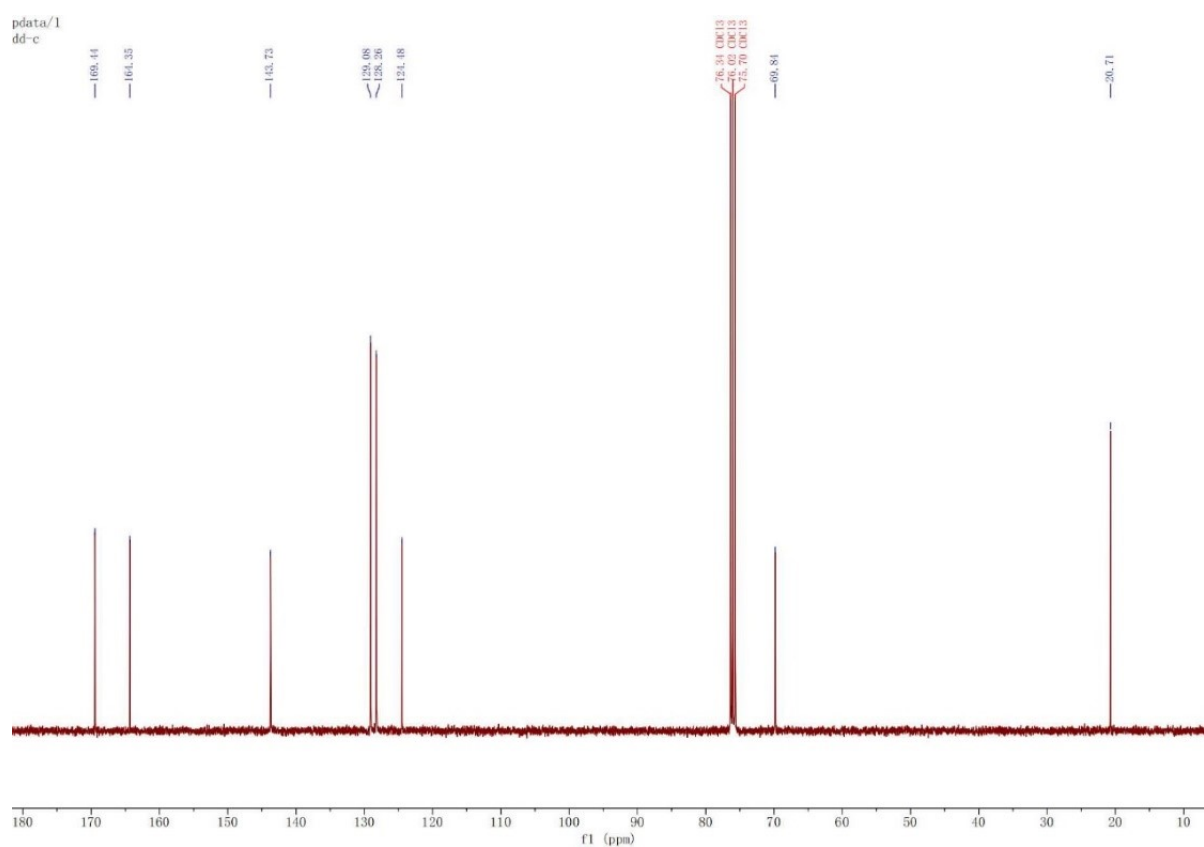


**Figure S21.** The  $^{13}\text{C}$ -NMR spectrum of **D-DTA** in  $\text{CDCl}_3$ .

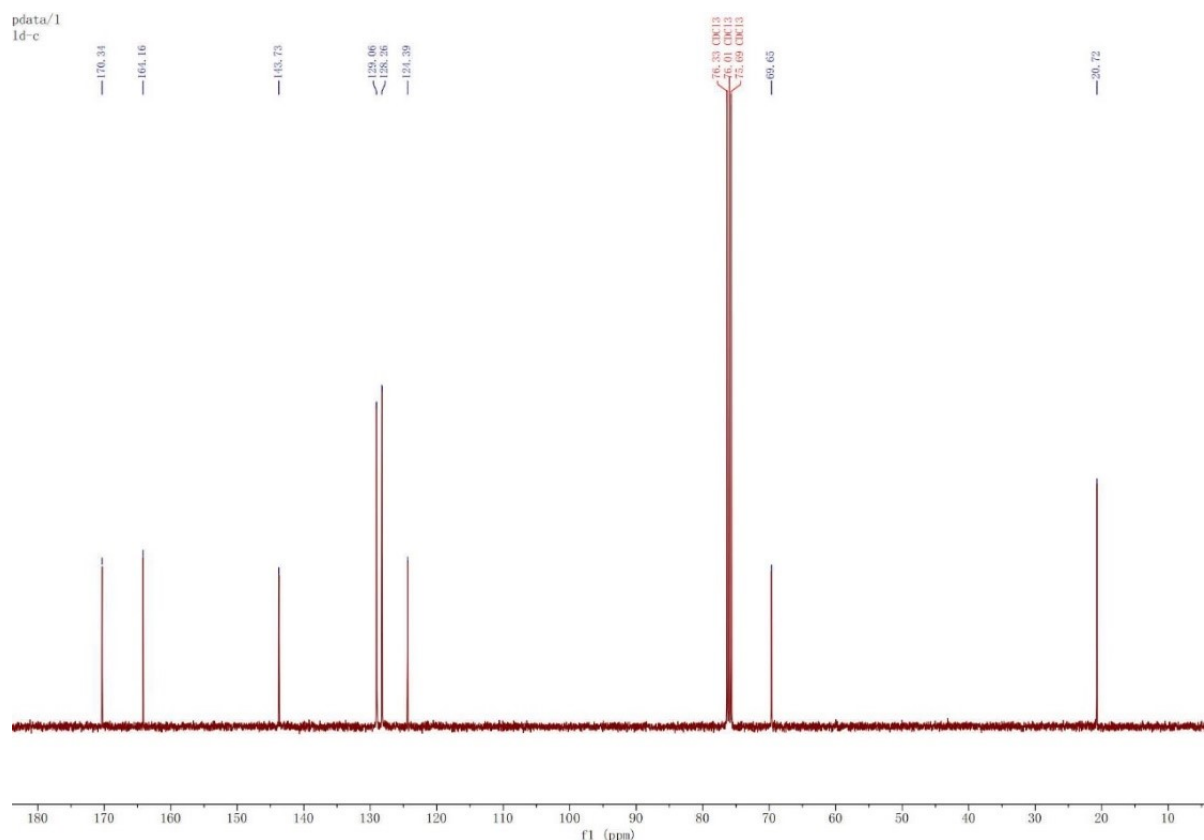


**Figure S22.** The  $^{13}\text{C}$ -NMR spectrum of **L-DTA** in  $\text{CDCl}_3$ .

D-TA #10 RT: 0.13 AV: 1 NL: 5.39E5  
T: FTMS {1,2} - p APCI corona Full ms [100.00-1000.00]

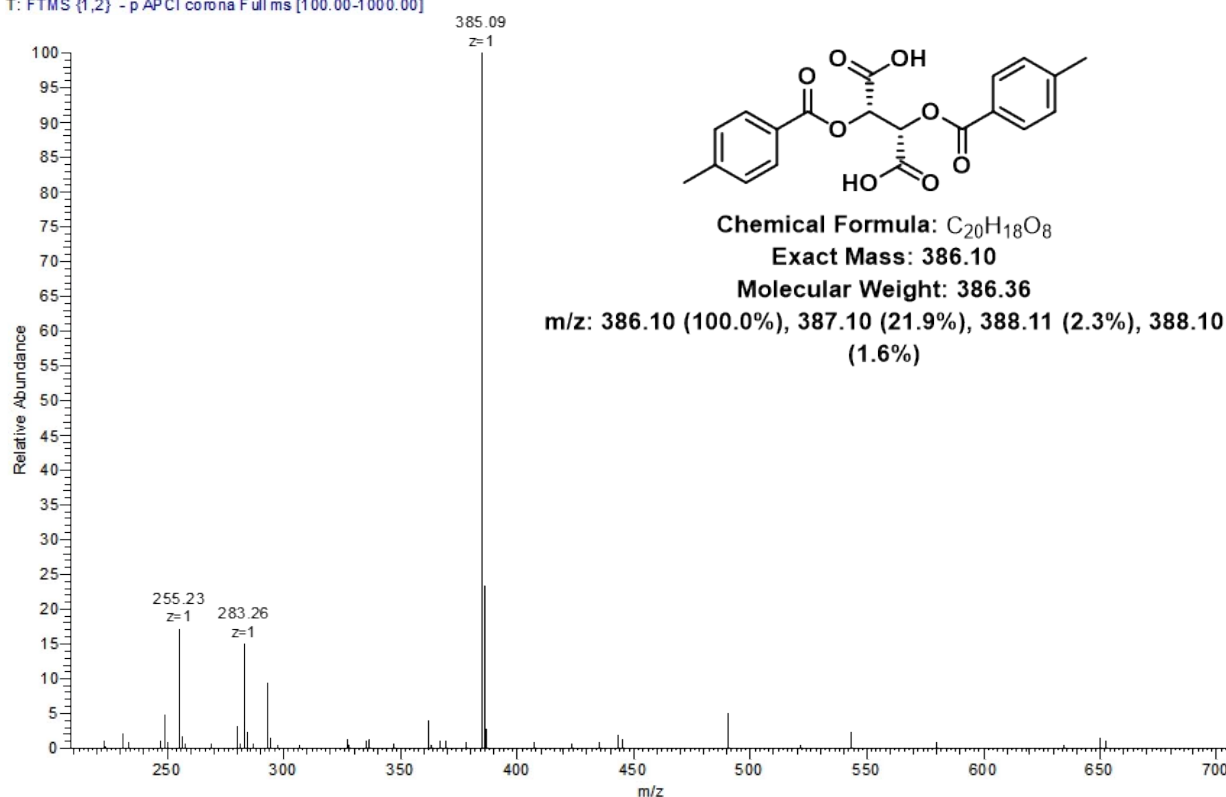


**Figure S23.** The mass spectrum of D-DTA.

L-TA#10 RT: 0.13 AV: 1 NL: 9.60E5  
T: FTMS {1,2} - p APCI corona Full ms [100.00-1000.00]

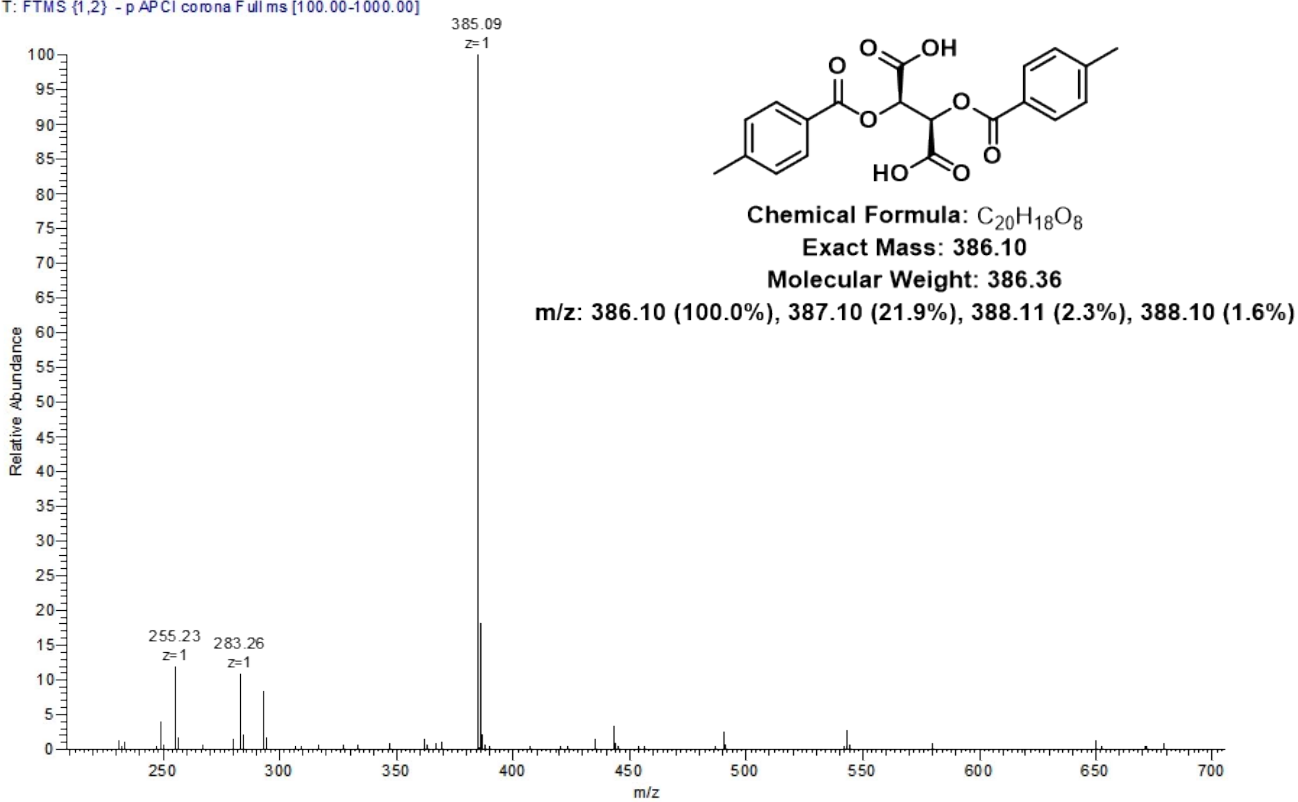


**Figure S24.** The mass spectrum of L-DTA.

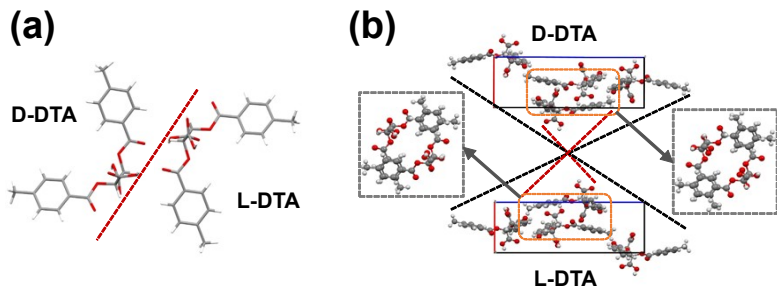


**Figure S25.** (a) The single crystal structure and (b) unit cell structure of the D- and L-DTA.

**Table S2.** Crystal data and structure refinement for D-DTA.

Identification code	D-DTA
Empirical formula	C <sub>20</sub> H <sub>18</sub> O <sub>8</sub>
Formula weight	386.36
Temperature/K	296
Crystal system	orthorhombic
Space group	P2 <sub>1</sub> 2 <sub>1</sub> 2 <sub>1</sub>
a/Å	7.9192(2)
b/Å	11.9987(3)
c/Å	21.8472(7)
α/°	90
β/°	90
γ/°	90
Volume/Å <sup>3</sup>	2075.92(10)
Z	4
ρ <sub>calc</sub> g/cm <sup>3</sup>	1.294
μ/mm <sup>-1</sup>	0.876
F(000)	848.0
Crystal size/mm <sup>3</sup>	0.22 × 0.15 × 0.13
Radiation	CuKα (λ = 1.54184)
2Θ range for data collection/°	8.094 to 152.162
Index ranges	-9 ≤ h ≤ 7, -13 ≤ k ≤ 15, -27 ≤ l ≤ 27
Reflections collected	12803
Independent reflections	3950 [R <sub>int</sub> = 0.0455, R <sub>sigma</sub> = 0.0370]
Data/restraints/parameters	3950/0/269
Goodness-of-fit on F <sup>2</sup>	1.053
Final R indexes [I>=2σ (I)]	R <sub>1</sub> = 0.0430, wR <sub>2</sub> = 0.1188
Final R indexes [all data]	R <sub>1</sub> = 0.0488, wR <sub>2</sub> = 0.1241
Largest diff. peak/hole / e Å <sup>-3</sup>	0.21/-0.17

Flack parameter	0.12(11)
-----------------	----------

**Table S3.** Crystal data and structure refinement for L-DTA.

Identification code	L-DTA
Empirical formula	C <sub>20</sub> H <sub>18</sub> O <sub>8</sub>
Formula weight	386.36
Temperature/K	296
Crystal system	orthorhombic
Space group	P2 <sub>1</sub> 2 <sub>1</sub> 2 <sub>1</sub>
a/Å	7.9208(2)
b/Å	11.9910(2)
c/Å	21.8333(4)
α/°	90
β/°	90
γ/°	90
Volume/Å <sup>3</sup>	2073.69(7)
Z	4
ρ <sub>calc</sub> g/cm <sup>3</sup>	1.295
μ/mm <sup>-1</sup>	0.877
F(000)	848.0
Crystal size/mm <sup>3</sup>	0.25 × 0.17 × 0.15
Radiation	CuKα (λ = 1.54184)
2Θ range for data collection/°	8.1 to 153.162
Index ranges	-7 ≤ h ≤ 9, -13 ≤ k ≤ 15, -27 ≤ l ≤ 27
Reflections collected	11693
Independent reflections	4001 [R <sub>int</sub> = 0.0246, R <sub>sigma</sub> = 0.0233]
Data/restraints/parameters	4001/6/257
Goodness-of-fit on F <sup>2</sup>	1.056
Final R indexes [I>=2σ (I)]	R <sub>1</sub> = 0.0394, wR <sub>2</sub> = 0.1070
Final R indexes [all data]	R <sub>1</sub> = 0.0431, wR <sub>2</sub> = 0.1108
Largest diff. peak/hole / e Å <sup>-3</sup>	0.13/-0.24
Flack parameter	-0.12(8)

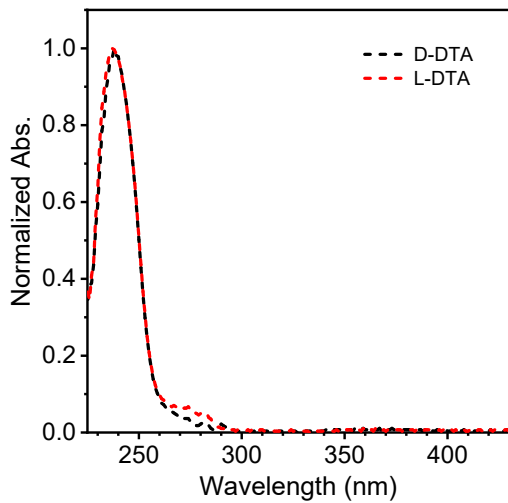


**Figure S26.** The UV-Vis absorption spectra of D- and L-DTA (the concentration is  $1 \times 10^{-5}$  M in THF).

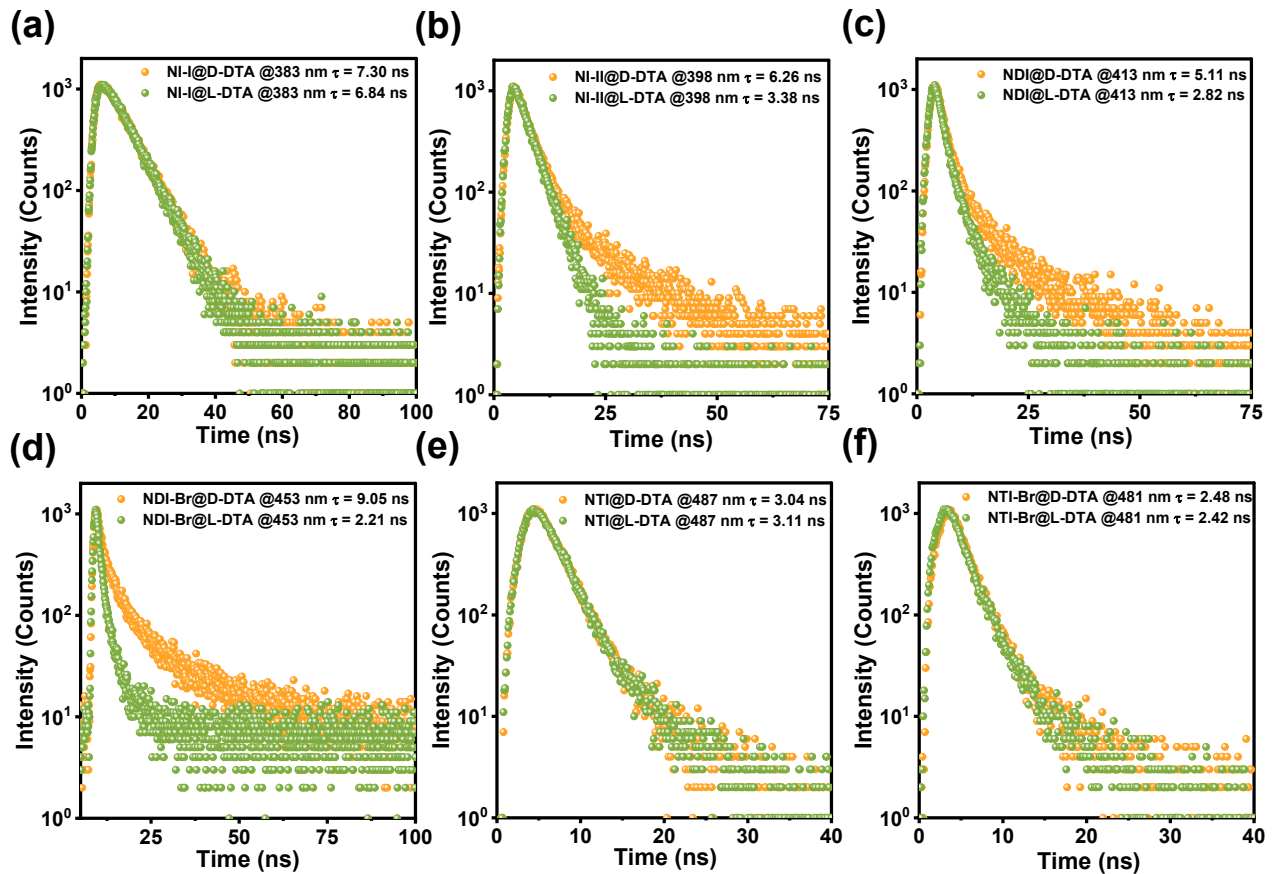


**Figure S27.** (a) The lifetime profiles of NI-I@D-DTA and L-DTA excited by 340 nm. (b) The lifetime profiles of NI-II@D-DTA and L-DTA excited by 340 nm. (c) The lifetime profiles of NDI@D-DTA and L-DTA excited by 360 nm. (d) The lifetime profiles of NDI-Br@D-DTA and L-DTA excited by 360 nm. (e) The lifetime profiles of NTI@D-DTA and L-DTA excited by 405 nm.

(f) The lifetime profiles of **NTI-Br@D-DTA** and L-DTA excited by 405 nm.

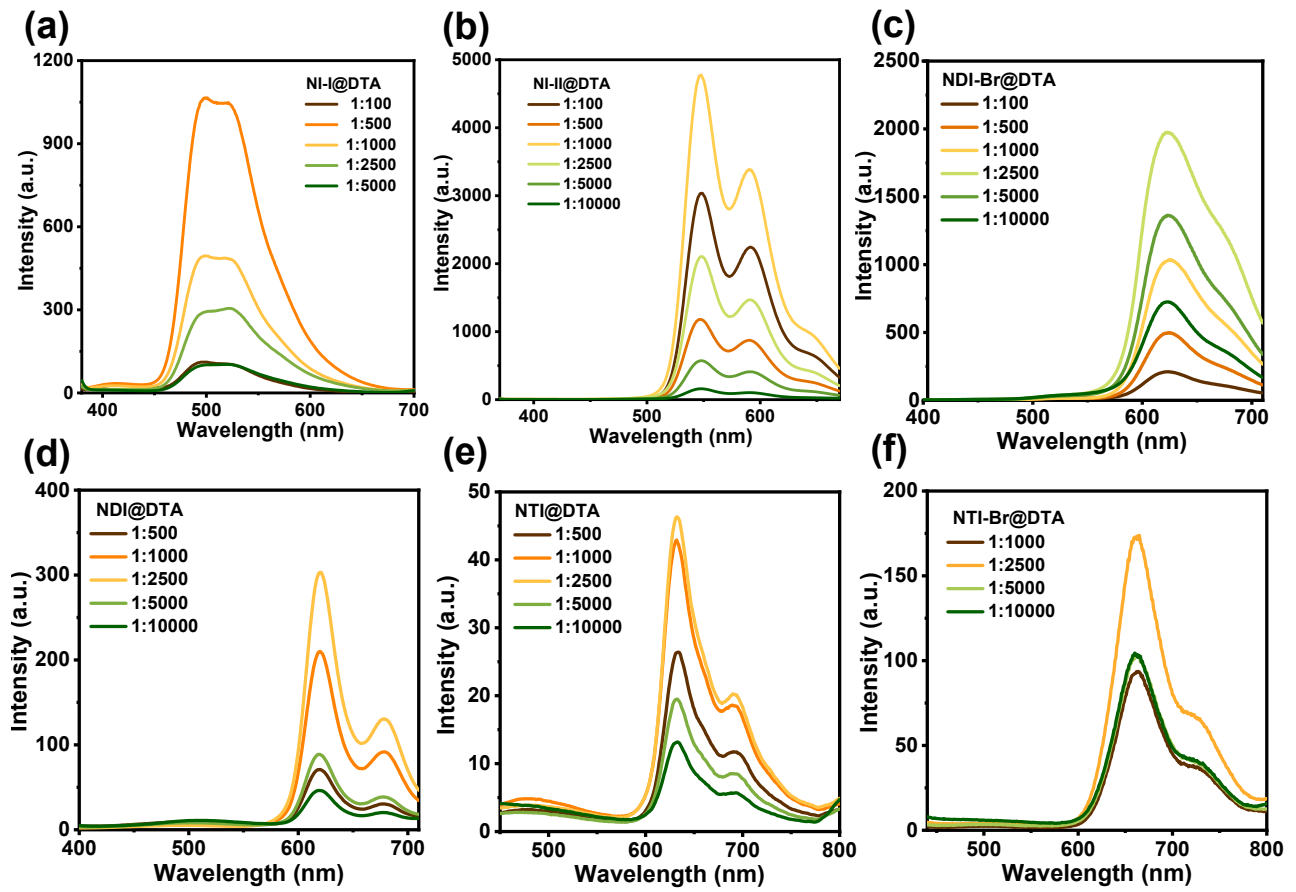


**Figure S28.** (a-f) The phosphorescence spectra of **NI-I**, **NI-II**, **NDI**, **NDI-Br**, **NTI**, and **NTI-Br@DTA** with different doping ratio, respectively (the **NI-I** and **NI-II@DTA** are excited by 340 nm, the **NDI** and **NDI-Br@DTA** are excited by 360 nm, **NTI** and **NTI-Br@DTA** are excited by 405 nm, and the delayed time is 50  $\mu$ s).

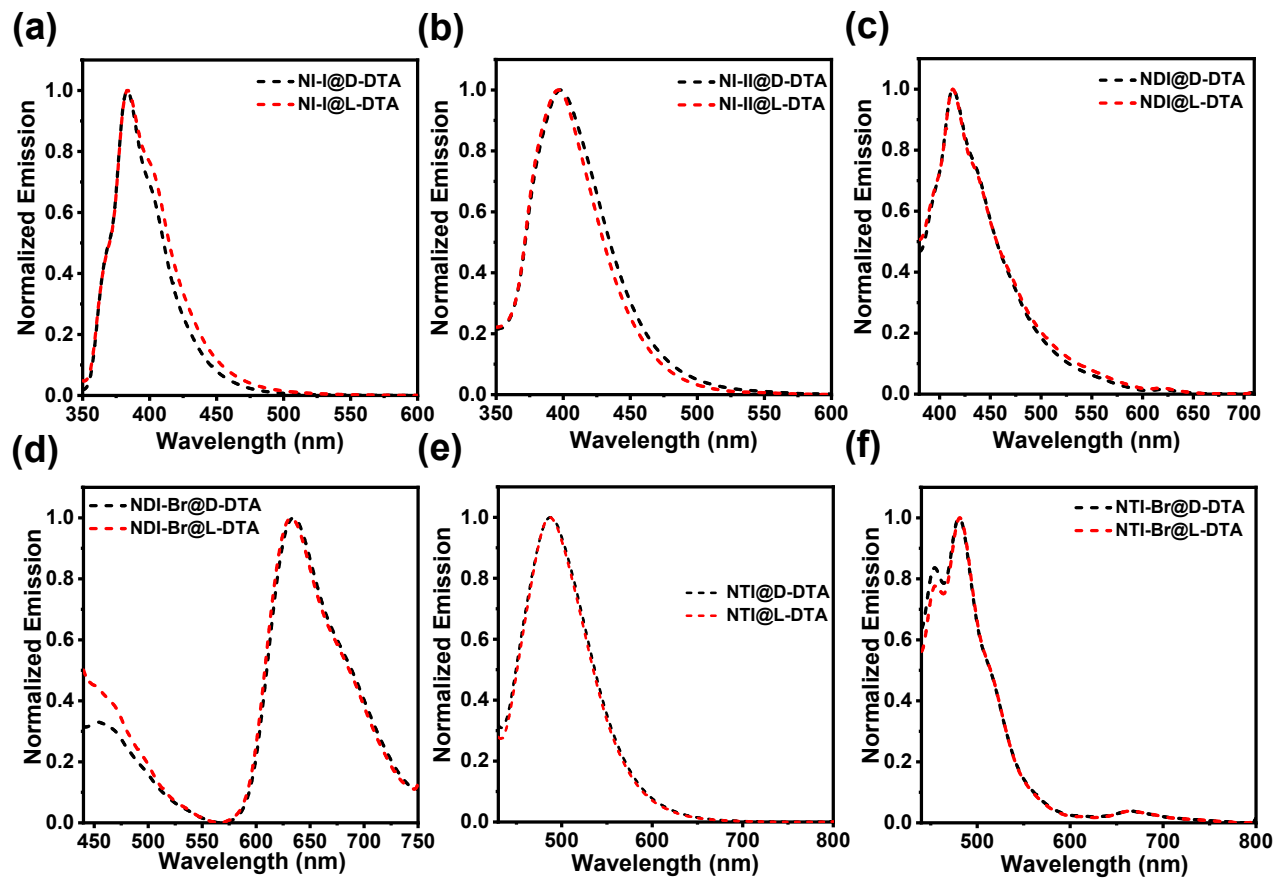


**Figure S29.** The fluorescence spectra of (a) **NI-I**, (b) **NI-II**, (c) **NDI**, (d) **NDI-Br**, (e) **NTI**, and (f) **NTI-Br@DTA** (the **NI-I** and **NI-II@DTA** are excited by 340 nm, the **NDI** and **NDI-Br@DTA** are excited by 360 nm, **NTI** and **NTI-Br@DTA** are excited by 405 nm).

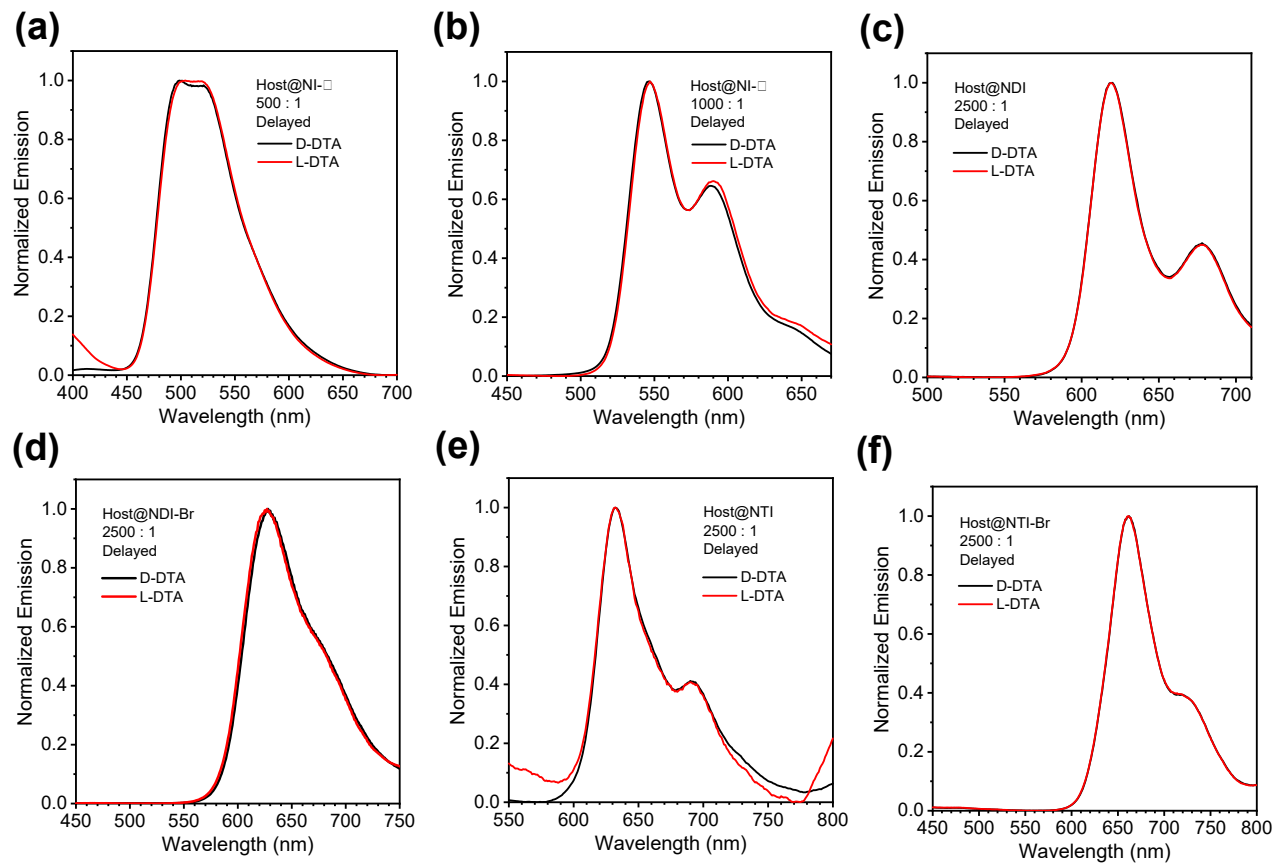


**Figure S30.** The phosphorescence spectra of (a) NI-I, (b) NI-II, (c) NDI, (d) NDI-Br, (e) NTI, and (f) NTI-Br@DTA (the NI-I and NI-II@DTA are excited by 340 nm, the NDI and NDI-Br@DTA are excited by 360 nm, NTI and NTI-Br@DTA are excited by 405 nm, and the delayed time is 50  $\mu$ s).

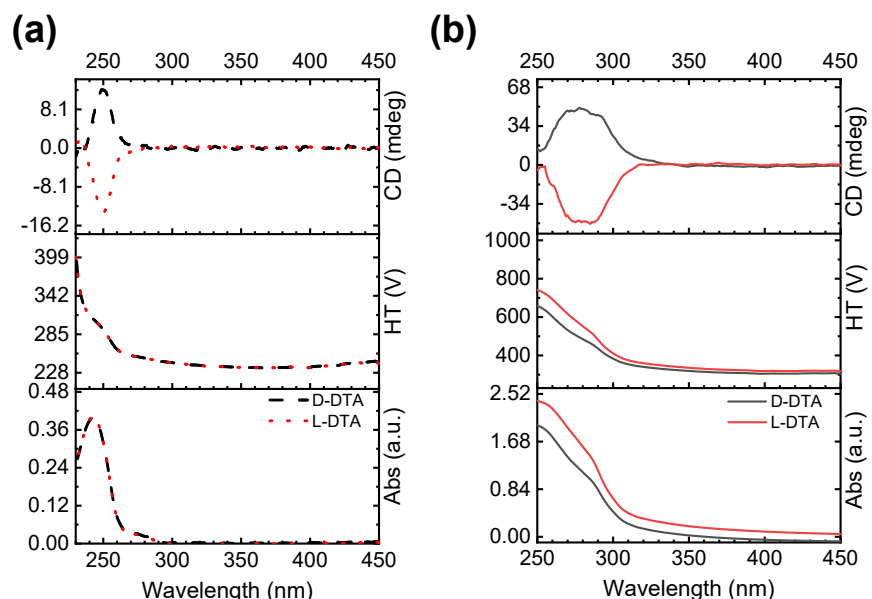


**Figure S31.** (a) The circular dichroism (CD) spectrum of L- and D-DTA (the concentration is  $1 \times 10^{-5}$  M).

<sup>5</sup> M in DCM). (b) The CD spectrum of L- and D-DTA (solid, KBr tableting, mass ratio: DTA:KBr = 1:500).

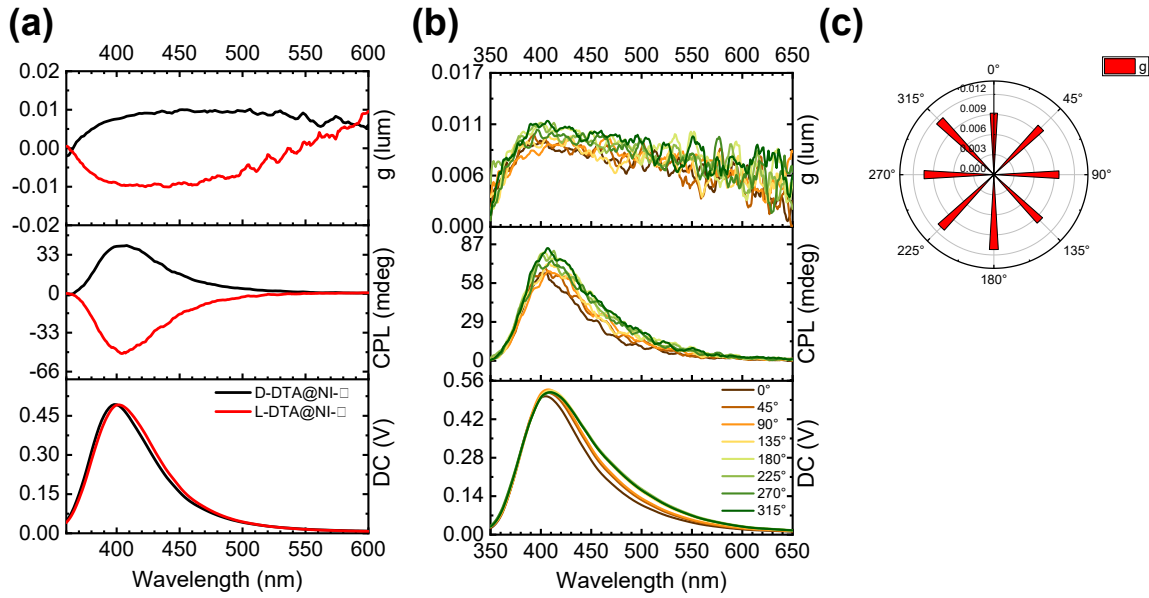


**Figure S32.** (a) The circularly polarized luminescence (CPL) spectrum of NI-I@DTA. (b) The CPL spectrum and (c) luminescence dissymmetry factor ( $g_{\text{lum}}$ ) of NI-I@DTA at different angles.

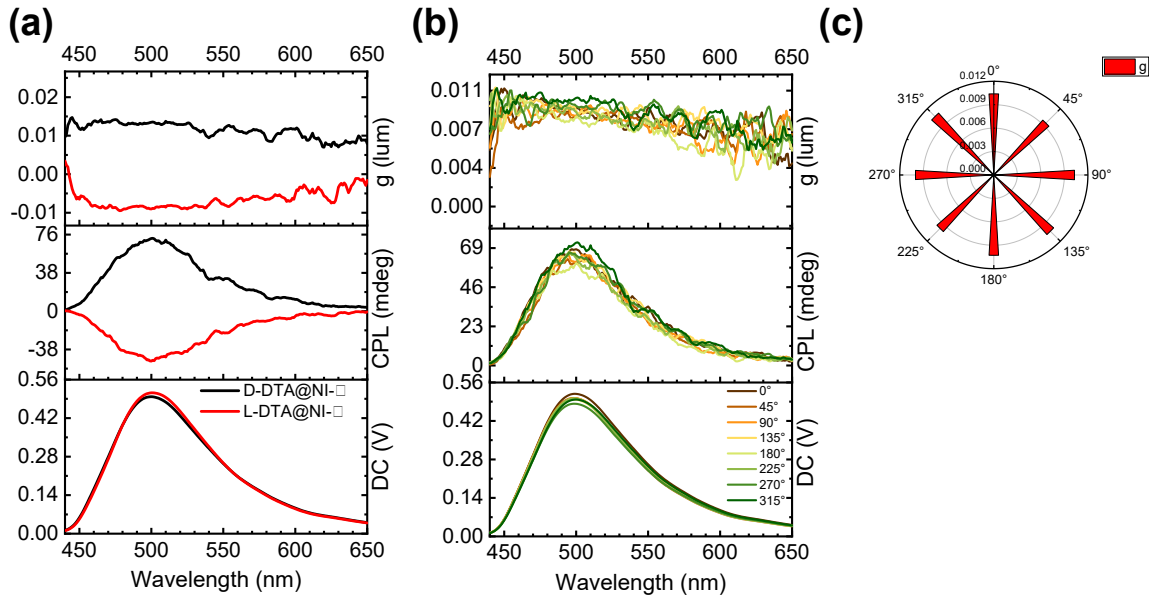


**Figure S33.** (a) The circularly polarized phosphorescence (CPP) spectrum of NI-I@DTA. (b) The CPP spectrum and (c)  $g_{\text{lum}}$  of NI-I@DTA at different angles.

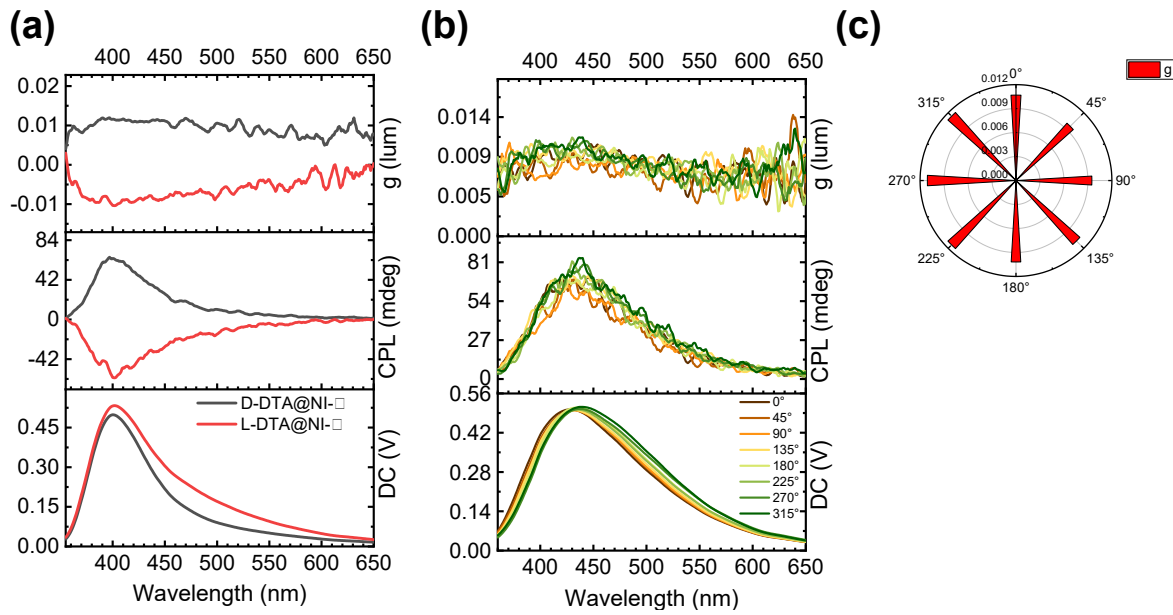


**Figure S34.** (a) The CPL spectrum of NI-II@DTA. (b) The CPL spectrum and (c)  $g_{\text{lum}}$  of NI-II@DTA at different angles.

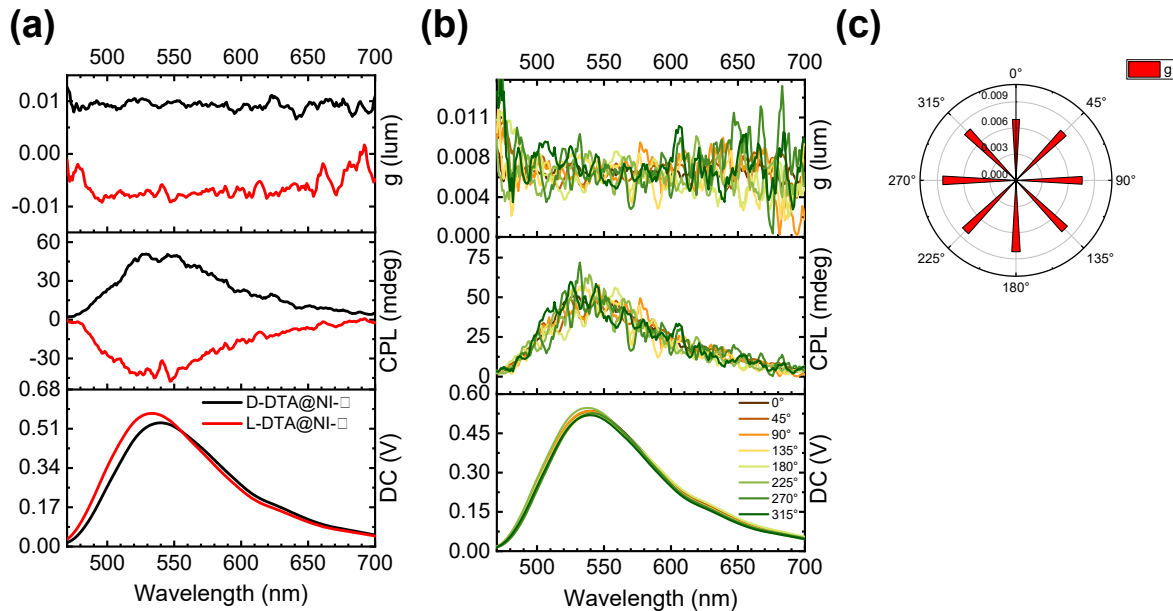


**Figure S35.** (a) The CPP spectrum of NI-II@DTA. (b) The CPP spectrum and (c)  $g_{\text{lum}}$  of NI-II@DTA at different angles.

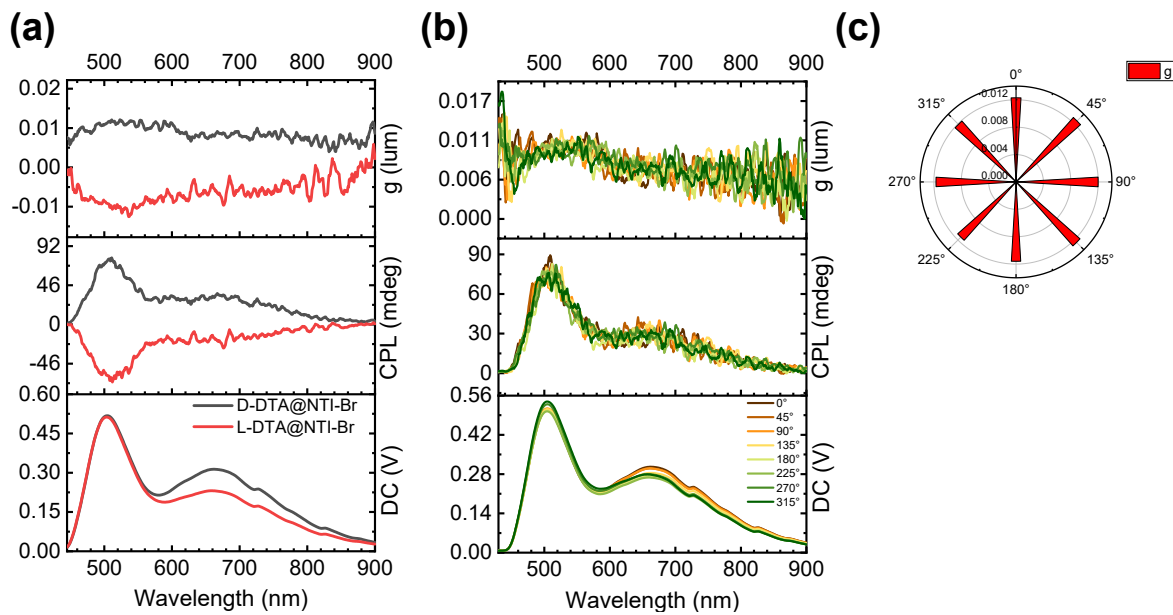


**Figure S36.** (a) The CPL spectrum of **NDI-Br@DTA**. (b) The CPL spectrum and (c)  $g_{\text{lum}}$  of **NDI-Br@DTA** at different angles.

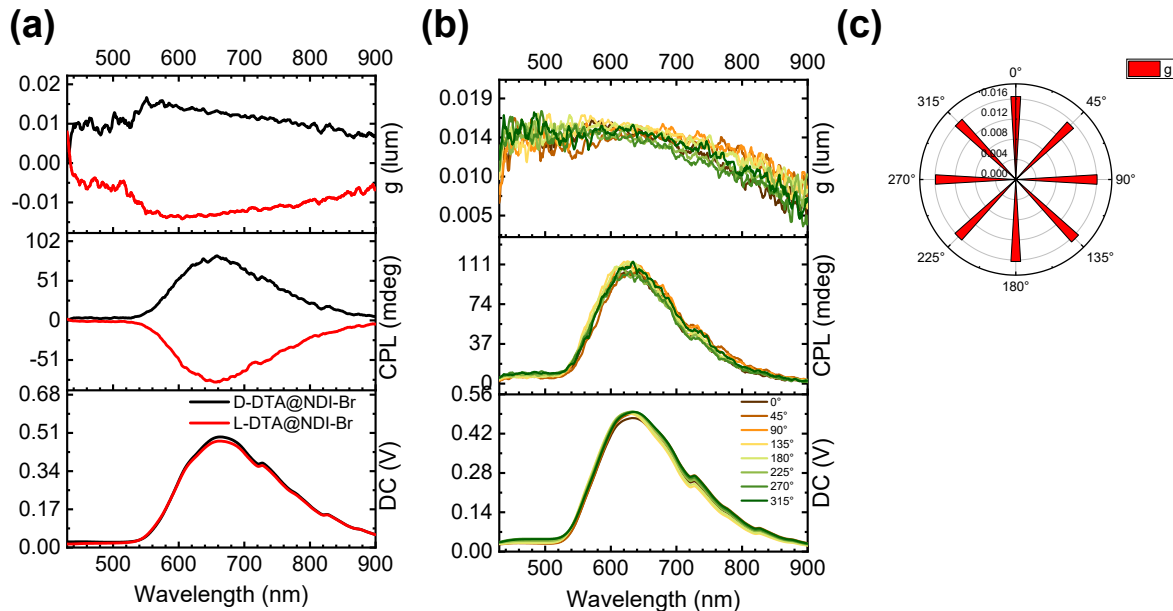


**Figure S37.** (a) The CPP spectrum of **NDI-Br@DTA**. (b) The CPP spectrum and (c)  $g_{\text{lum}}$  of **NDI-Br@DTA** at different angles.

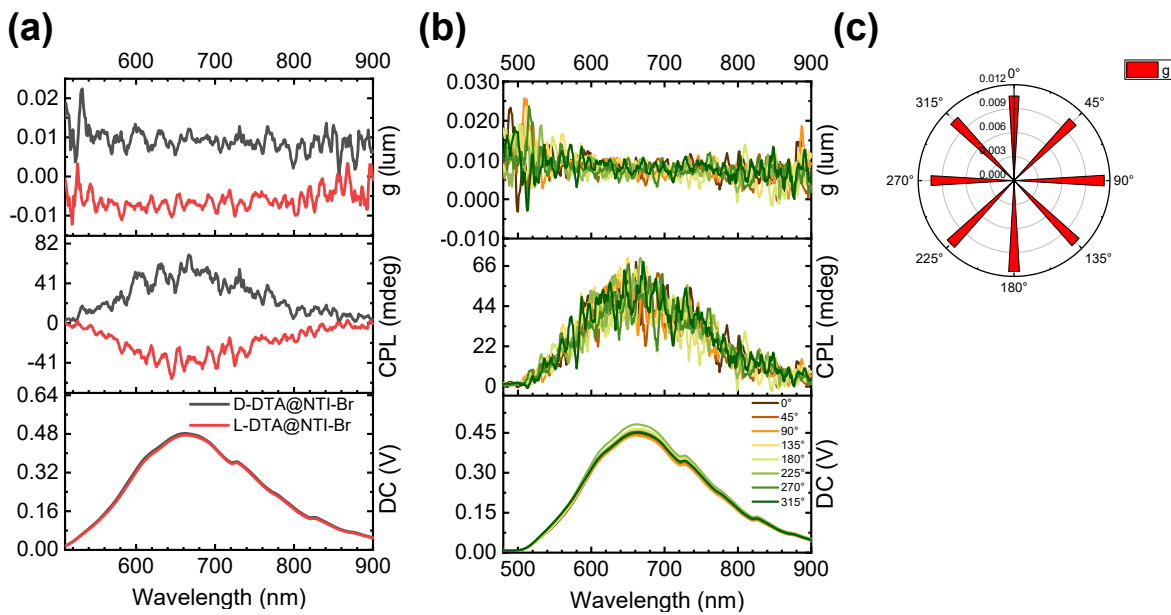


**Figure S38.** (a) The CPL spectrum of **NTI-Br@DTA**. (b) The CPL spectrum and (c)  $g_{lum}$  of **NTI-Br@DTA** at different angles.

## References

- [1] G.-T. Wen, M.-Z. Zhu, Z. Wang, X.-M. Meng, H.-Y. Hu, Q.-X. Guo, *Chin. J. Chem.* **2006**, *24*, 1230.
- [2] S. Kuila, A. Ghorai, P. K. Samanta, R. B. K. Siram, S. K. Pati, K. S. Narayan, S. J. George, *Chem. Eur. J.* **2019**, *25*, 16007.
- [3] H. Ning, G. Zhang, H. Chen, Z. Wang, S. Ni, F. Lu, F. Liu, L. Dang, J. Liu, F. He, Q. Wu, *Chem. Mater.* **2021**, *33*, 1976.
- [4] G. Zhang, H. Ning, H. Chen, Q. Jiang, J. Jiang, P. Han, L. Dang, M. Xu, M. Shao, F. He, Q. Wu, *Joule* **2021**, *5*, 931.
- [5] J. Morgan, Y. J. Yun, A. J.-L. Ayitou, *Photochem. Photobiol.* **2022**, *98*, 57.
- [6] A. J. Ghielmetti, C. Barner-Kowollik, F. E. Du Prez, H. A. Houck, *Polym. Chem.* **2023**, *14*, 1554.